THERMODYNAMIC ASPECTS OF SUPERCRITICAL FLUIDS PROCESSING: APPLICATIONS TO POLYMERS AND WASTES TREATMENT

F. CANSELL and S. REY

CNRS, Université Bordeaux I[1]

P. BESLIN

APESA[2]

ASPECTS THERMODYNAMIQUES DES PROCÉDÉS METTANT EN ŒUVRE DES FLUIDES SUPERCRITIQUES : APPLICATIONS AUX TRAITEMENTS DES POLYMÈRES ET DES DÉCHETS

La mise en œuvre des fluides supercritiques est d'un intérêt croissant dans de nombreux domaines : pour la séparation (séparation et purification en pétrochimie, industrie alimentaire) et la chromatographie par fluides supercritiques (séparation analytique et préparatoire, détermination des propriétés physicochimiques), comme milieux réactifs aux propriétés continûment ajustables allant du gaz au liquide (polyéthylène de faible densité, élimination des déchets, recyclage des polymères), en géologie et en minéralogie (volcanologie, énergie géothermique, synthèse hydrothermique), dans la formation des particules, fibres et substrats (produits pharmaceutiques, explosifs, revêtements), pour le séchage des matériaux (gels).

Cet article présente les propriétés physicochimiques exceptionnelles des fluides supercritiques en rapport avec leurs applications en ingénierie. Après un bref rappel des concepts fondamentaux relatifs au comportement critique des fluides purs, nous développons d'une manière plus détaillée les propriétés physicochimiques ajustables des fluides dans le domaine supercritique. La deuxième partie de l'article décrit les applications en ingénierie des fluides supercritiques relatives aux réactions chimiques et au traitement des polymères. Chaque présentation d'application est divisée en deux parties : la première rappelle les concepts de base et le contexte général ainsi que les propriétés physicochimiques, la seconde développe les applications en ingénierie se rapportant au domaine concerné.

THERMODYNAMIC ASPECTS OF SUPERCRITICAL FLUIDS PROCESSING: APPLICATIONS TO POLYMERS AND WASTES TREATMENT

Supercritical fluid processes are of increasing interest for many fields: in supercritical fluid separation (petroleum-chemistry separation and purification, food industry) and supercritical fluid chromatography (analytical and preparative separation, determination of physicochemical properties); as reaction media with continuously adjustable properties from gas to liquid (low-density polyethylene, waste destruction, polymer recycling); in

(1) Institut de chimie de la matière condensée de Bordeaux
Château Brivazac,
33608 Pessac Cedex - France

(2) Pôle Environnement Sud Aquitaine,
Hélioparc,
64000 Pau - France

geology and mineralogy (volcanoes, geothermal energy, hydrothermal synthesis); in particle, fibber and substrate formations (pharmaceuticals, explosives, coatings); in drying materials (gels).

This paper presents the unusual physicochemical properties of supercritical fluids in relation to their engineering applications. After a short report of fundamental concepts of critical behavior in pure fluids, we develop in more details the tunable physicochemical properties of fluid in the supercritical domain. The second part of this paper describes the engineering applications of supercritical fluids relevant of chemical reactions and polymer processing. Each application presentation is divided in two parts: the first one recalls the basic concepts including general background, physicochemical properties and the second one develops the engineering applications relevant of the advocated domain.

ASPECTOS TERMODINÁMICOS DEL TRATAMIENTO DE LOS FLUIDOS SUPERCRÍTICOS : APLICACIONES PARA LOS TRATAMIENTOS DE LOS POLÍMEROS Y DE LOS RESIDUOS

La implementación de los fluidos supercríticos presenta un interés cada vez mayor en numerosos campos : para la separación (separación y purificación en petroquímica, industria alimentaria) y la cromatografía de los fluidos supercríticos (separación analítica y preparatoria, determinación de las propiedades fisicoquímicas) ; en los medios reactivos con propiedades continuamente ajustables, que van desde el gas líquido (polietilenos de baja densidad, eliminación de los residuos, reciclado de los polímeros) ; en geología y en mineralogía (vulcanología, energía geotérmica, síntesis hidrotérmica) ; en la formación de partículas, fibras y substratos (productos farmacéuticos, explosivos, revestimientos) ; para los materiales deshidratantes (geles).

En este artículo se presentan las excepcionales propiedades fisicoquímicas de los fluidos supercríticos con respecto a sus aplicaciones en ingeniería. Tras un breve resumen de los conceptos fundamentales relativos al comportamiento crítico de los fluidos puros, hemos desarrollado con mayor detalle las propiedades fisicoquímicas ajustables de los fluidos en el aspecto supercrítico. En la segunda parte del artículo se describen las aplicaciones en ingeniería de los fluidos supercríticos relativas a las reacciones químicas y para el tratamiento de los polímeros : en la primera se hacen destacar los conceptos básicos y el contexto general así como las propiedades fisicoquímicas y, en la segunda parte, se desarrollan las aplicaciones en ingeniería referentes al aspecto correspondiente.

INTRODUCTION

The capability of some supercritical fluids to replace toxic industrial solvents, the ability of tuning solvent characteristics for highly specific separation or reactions and the possibility to make new materials at mild conditions are the main considerations which lead to the current industrial and scientific interest in supercritical fluids. Often viewed as “dense gases”, these fluids possess physicochemical properties, such as density, viscosity or diffusivity, which are intermediate between those of liquids and gases, as outlined in Table 1.

TABLE 1

Characteristic magnitudes of thermophysical properties of fluids

	Liquid	Supercritical	Gas*
ρ ($kg \cdot m^{-3}$)	1000	100-800	1
η ($Pa \cdot s$)	10^{-3}	10^{-5}-10^{-4}	10^{-5}
D$^\blacklozenge$ ($m^2 \cdot s^{-1}$)	10^{-9}	10^{-8}	10^{-5}

Symbols used: ρ for density; η for viscosity; D for diffusion coefficient: * at ambient conditions; $^\blacklozenge$ for small-molecule solute.

Supercritical fluid processes are of increasing interest for many fields [1] such as supercritical fluid separation (petroleum-chemistry separation and purification, food industry) [2, 3, 4, 5] and supercritical fluid chromatography (analytical and preparative separation, determination of physicochemical properties) [6] and [7]. Supercritical fluids are used as reaction media with continuously adjustable properties from gas to liquid (low-density polyethylene, waste destruction, polymer recycling) [8, 9, 10, 11, 12, 13], in geology and mineralogy (volcanoes, geothermal energy, hydrothermal synthesis) [14], in formation of particles, fibbers and substrates (pharmaceuticals, explosives, coatings) [15, 16, 17, 18] or in drying materials (gels) [19] and [20].

The further development of supercritical fluid applications depends both on the ability to exploit their unusual properties towards making products with characteristics and specifications that cannot be obtained by other means and on the evolution of financial, legislative and even psychological aspects which may become decisive elements. In this paper, we present the unusual physicochemical properties of

supercritical fluids in relation to their engineering applications. After a short report of fundamental concepts of critical behavior in pure fluids, we develop in more details the tunable physicochemical properties of fluids in the supercritical domain. The second part of this paper describes the engineering applications of supercritical fluids relevant to watses treatment and polymer processing. Each application presentation is divided in two parts: the first one recalls the basic concepts including general background and physico-chemical properties, the second one develops the engineering applications relevant to the advocated domain.

1 CRITICAL AND SUPERCRITICAL BEHAVIOR OF FLUIDS

1.1 Critical behavior of pure fluids

The state of homogeneous pure fluid can be described by variables or functions of state, such as pressure (P), temperature (T) and molar volume (V) which are not independent variables. The Equation of State (EoS) $f(P, T, V) = 0$ lies these variables. In the P, V, T three-dimensional space this EoS is represented by a surface as shown in Figure 1.

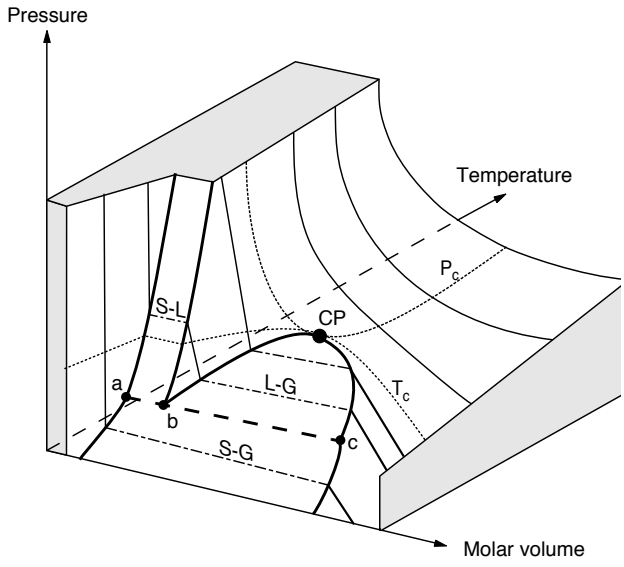

Figure 1

Schematic representation of phase surface in P, V, T space for a pure compound. The abc line corresponds to the solid, liquid and gas coexistence. *CP* is the critical point; T_c is the critical temperature; P_c is the critical pressure.

Each point of this surface corresponds to a state of the system. Generally, to study the thermodynamic behavior of a system, it is easier to use only two variables and so to work in a two-dimensional space such as (P, V) (Clapeyron diagram) or (P, T) (see section 1.2, Fig. 3).

On the phase surface presented on Figure 1, the supercritical domain corresponds to a pressure and a temperature superior to the critical coordinates of the pure fluid (P_c, T_c). It is easy to define the limits between the solid state surface and the gas and liquid state surfaces on the coexistence domain. However, if the critical point is rounded, the transition from liquid to gas phase is continuous and without any phase transition. So in this paper, we use liquid and gas notation on the liquid-gas coexistence domain and fluid notation for the entire P, V, T surface (excepted solid state surface).

The critical point (*CP*) of a pure fluid is defined by: i) the disappearance of the difference between gas and liquid; ii) the divergence of compressibility; iii) the phenomenon of critical opalescence.

The phenomenon (ii) is expressed by the conditions:

$$(\partial P/\partial V)_T = 0 \quad \text{and} \quad (\partial^2 P/\partial V^2)_T = 0 \qquad (1)$$

which evidence the divergence of the isothermal compressibility $K_T = (-1/V)\ (\partial V/\partial P)_T$. At the critical density and at a few Celsius degrees from the critical temperature, K_T is much higher than that of a perfect gas at the same density [21]. So near the critical point, large density fluctuations can be generated at low cost in free energy. Table 2 presents, in the case of pure water, the density and K_T variations at 24 MPa as a function of temperature [22]. A temperature variation of 20°C can divide the density by three and K_T quickly increases of three orders of magnitude up to the vicinity of the critical point and then slowly decreases.

TABLE 2

Evolution of density (ρ), isothermal compressibility (K_T) of pure water at 24 MPa as a function of temperature. ΔP is the pressure variation of the closed system obtained for a volume variation of 1% as a function of the isothermal compressibility (critical coordonates of pure water: T_c = 374.1°C; P_c = 22.1 MPa; ρ_c = 317 kg.m^{-3}) [22]

T (°C)	50	250	380	400	500	600
ρ (kg.m^{-3})	998	820	372	148	85.2	67.6
K_T (MPa^{-1})	4.5 10^{-4}	1.2 10^{-3}	0.48	0.11	0.054	0.047
ΔP (MPa)	22	8.3	0.021	0.093	0.19	0.21

In order to understand the mechanical behavior of supercritical fluids, K_T evolution is related to the pressure variation (ΔP) induced by 1% volume reduction of the system (Table 2). ΔP evolution, apart from the vicinity of the critical point, evidences that a supercritical fluid is not much compressible and can be used as a reactive or mass-transfer fluid for material processing.

K_T is proportional to the mean squared density fluctuations and can be related to the pair correlation function *G(r)* which is the ratio of local to bulk density at a distance *r* from a molecule fixed at the origin.

The function *G(r)* equals 0 inside the hard core of repulsion of the molecule at the origin and approaches the unit at large distance. The exact relation between the spatial integral of *G(r)* and K_T is expressed as follows [23]:

$$RT\rho K_T = 1 + \rho \int G(r)dr \qquad (2)$$

where *R* is the perfect gas constant.

Figure 2 shows the schematic evolution of *G(r)* in liquid, gas and fluid near the critical point. For liquids, this function shows pronounced oscillations indicating the arrangement of several shells of neighbors around a given molecule [24] and [25].

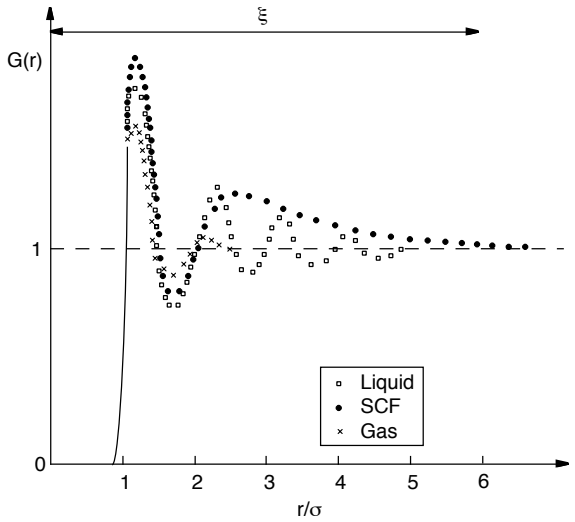

Figure 2

Schematic representation of the pair correlation function in liquid, gas and supercritical fluid. σ is the molecular diameter, ξ is the correlation lenght and *G(r)* is the ratio of local to bulk density (adapted from [21, 24, 25]).

For gases, after the first shell, the local density becomes equal to the bulk density. In fluids, the divergence of K_T at the critical point leads to the important consequence that the integral of *G(r)* diverges (Fig. 2).

The correlation function develops a long "tail" which is a signature of approaching criticality [21]. This criticality implies the existence of long range correlation, well beyond the extent of the range of molecular potentials. The long ranged correlations, which induce higher K_T variations, influence the rate of change of solubility with respect to temperature and pressure. On the other hand, the structure of the first shell is short-range and is unrelated to criticality. The solvation effects due to molecular disparity are short-range and they control the absolute solubility [26].

The range of density fluctuations is measured by the quantity ξ called correlation length (Fig. 2). *G(r)* near but not at the critical point is proportional to $\exp(-r/\xi)/r$ and on the critical isochor ($\rho = \rho_c$) we have [21]:

$$\xi = \xi_0 \left| \Delta T^* \right|^{-\gamma} \qquad (3)$$

with the classical value of the exponent γ equal to 0.5 and $\Delta T^* = (T - T_c/T_c)$.

For carbon dioxide (CO_2), ξ is 1.3 nm at 10°C above T_c and 5.5 nm at 1°C above T_c [27]. These values are to be compared with the molecular size of 0.4 nm and with the average intermolecular distance of 0.55 nm at ρ_c. The excess values of ξ at 1°C from the critical point in comparison with the intermolecular distance explain the universal fluid behavior near the critical point.

In conclusion, the divergence of K_T, which is related to a density gradient of several percent in the vicinity of the critical point, does not allow process developments in *P-T* domain very close to this point. On the contrary, the tunable characters of supercritical fluids, in the ranges from a few °C to $2T_c$ and a few 0.1 MPa to $3P_c$, are interesting in their commercial exploitation.

1.2 Behavior of supercritical fluids and their mixtures

The critical temperature (T_c), pressure (P_c) and density (ρ_c) for fluids commonly used in supercritical fluid processes and studies are listed in Table 3 [28].

TABLE 3

Critical coordinates of usual pure fluids in supercritical fluid processes. T_c, P_c and ρ_c are the critical temperature, pressure and density, respectively [28]

Fluid	T_c (°C)	P_c (MPa)	ρ_c (kg·m^{-3})
Carbon dioxide	31.2	7.38	468
Nitrogen dioxide	36.4	7.24	457
Ammonia	132.4	11.29	235
Water	374.1	22.1	317
Ethylene	9.5	5.06	220
Ethane	32.5	4.91	212
Propane	96.8	4.26	225
n-Pentane	196.6	3.37	232
Cyclohexane	279.9	4.03	270
Benzene	289.5	4.92	304
Toluene	320.8	4.05	290
Methanol	240.0	7.95	275
Ethanol	243.1	6.39	280
Isopropanol	235.6	5.37	274
Acetone	235.0	4.76	273

CO_2, which has a T_c near the ambient temperature and a P_c not much higher, is used as a solvent in most of the supercritical fluid processes. Water, which has much higher T_c and P_c, is used in Austin in an industrial process for wastes treatment [29] and frequently in reaction studies because of its potential practical applications in reactive processes at supercritical conditions. In order to point out the possibility of tuning fluid density in the vicinity of the critical point, we present in Figure 3 the isochore evolution of pure water in the (*P, T*) diagram. This figure shows that the fluid density can be adjusted of one order of magnitude for pressure or temperature variations of 20 MPa or 200°C respectively. This behavior can be reported in first approximation for every fluid using the reduced coordinates such as $T^* (T/T_c)$ and $P^* (P/P_c)$.

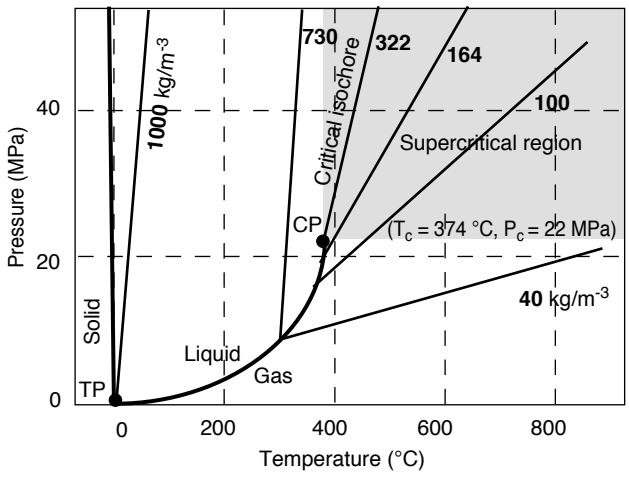

Figure 3

Phase diagram of pure water (adapted from [22]). *TP* is the triple point and *CP* is the critical point.

More generally, the tunable fluid characteristics are reported in Table 4 for pure water as an example.

TABLE 4

Evolution of density (ρ),viscosity (η) and relative static permittivity (ε_r) of pure water as a function of temperature and pressure [22]

T (°C) *P* (MPa)	25 10	400 30	150 0.1
ρ (kg·m^{-3})	999	353	0.52
η (Pa·s)	90 10^{-5}	4.5 10^{-5}	1 10^{-5}
ε_r	78.9	5.9	1.5

The supercritical fluid processes generally involve the contact between a packed bed of solid phase (or viscous liquid) and the fluid, and require knowledge of equilibrium solubilities and component selectivities (thermodynamic data) as well as mass transfer rates (kinetic data). The different behavior of fluid density and viscosity induces that the relative importance of natural convection (as measured by the ratio of buoyancy to inertial forces) is two orders of magnitude higher in a supercritical fluid than in a liquid (at constant Reynolds number). Indeed, the kinematic viscosity $\nu = \eta/\rho$ (η = dynamic viscosity and ρ = density of fluid) is very low in the supercritical region which is important

for mass transfer applications, since natural convection effects are inversely proportional to the square of the kinematic viscosity [30].

1.2.1 Solute solubility

The solute solubility in a dilute binary mixture is important for supercritical fluid processes. The solute is generally much less volatile and has a larger size than the solvent, which involves attractive mixture in the useful classification scheme (attractive, repulsive and weakly attractive) [31].

The solubility profile of a solute in a supercritical fluid significantly changes with pressure and temperature. It can be directly related to the pressure and temperature, based on fugacities [32], solubility parameters [33], virial coefficients [34, 35, 36] and fluid density [37].

In this paper we develop successively the first and the last relations. The first relation permits to relate the solubility to the critical behavior of fluids and the last one is very easy to use in chemical engineering process.

The general solubility equation based on fugacities which characterize the solubility of a solid solute in a supercritical fluid is expressed as follows:

$$Y_2 = \frac{P_2^s}{P}\frac{1}{\varphi_2^f}\varphi_2^s \exp\int_{P_2^s}^{P}\frac{V_2}{RT}dP \qquad (4)$$

where Y_2 is the mole fraction of solute, P_2^s is the solute saturation pressure which only depends on temperature; V_2 is the solute molar volume in the solid phase, φ_2^s is the fugacity coefficient of solute at the saturation pressure and φ_2^f is the fugacity coefficient of solute in fluid phase ($f_2^f = Y_2\,\varphi_2^f\,P$ = fugacity of the solute in fluid phase).

Considering that the solute is a pure solid, φ_2^s is equal to 1 at P_2^s, V_2 is a constant in the studied pressure range [38] and Y_2 is expressed by:

$$Y_2 = \frac{P_2^s}{P}\frac{1}{\varphi_2^f}\exp\frac{V_2\left(P - P_2^s\right)}{RT} \qquad (5)$$

The first term in Equation 5 corresponds to the solute solubility in gas phase (Dalton's law). The second one takes into account the interactions between the solute and its molecular environment, and the third one takes into account the hydrostatic pressure effect on the solid phase fugacity $\left(f_2 = P_2^s \exp(V_2(P - P_2^s)/RT)\right)$.

The solute solubility, which is a function of the density as shown in Figure 4 [39], can be expressed by the ratio of the real solubility in supercritical fluid to the gas solubility (so called enhancement factor *E*):

$$E = Y_2 / \left(P_2^s / P\right) = \frac{1}{\varphi_2^f}\exp\frac{V_2\left(P - P_2^s\right)}{RT} \qquad (6)$$

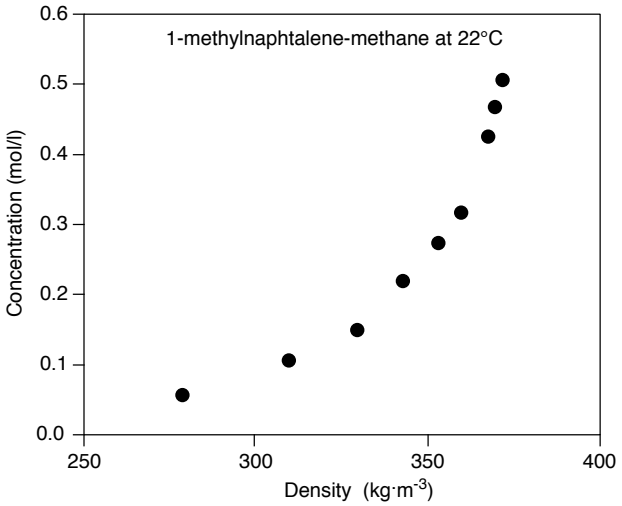

Figure 4

Solubility of 1-methylnaphtalene in methane at 22°C versus density of the mixture (adapted from [39]).

E factor increases with the size of the solute, which indicates that the solvation forces are in relation to the molecule number in interaction with the solute. Solutes with a same size but a different polarity present an equivalent factor *E*. Finally, *E* factor is very sensitive to the nature of the solvent and may vary to 8 orders of magnitude as a function of density [38]. The classical description takes into account short-range effects in relation to solvation phenomena, and long-range correlations due to local quasicriticality, that leads to large partial molar properties in the vicinity of the critical point [40, 41, 42, 43].

In order to understand the solid solubility in supercritical fluids, it is necessary to understand the fugacity coefficient evolution as a function of composition and density.

The fugacity coefficient is defined and calculated by:

$$\ln \varphi_2^f = \int_0^P \left(\frac{V_2^f}{RT} - \frac{1}{P} \right) dP \tag{7}$$

where V_2^f is the partial molar volume of the solute in fluid phase and can be expressed as:

$$V_2^f = V K_T \, n \left(\partial P / \partial n_2 \right)_{T,P} \tag{8}$$

where V is the molar volume of the solvent, n is the total number of moles in the mixture and n_2 is the number of moles of the solute.

The partial molar volume is a macroscopic property and physically corresponds to the volume of solute to add in the mixture in order to maintain P and T at constant values (per mole of solute). In the liquid, the partial molar volume is equal to a few cm^3 per mole which corresponds to one core of solvation around the solute. The solute partial molar volumes are very large and negative in the highly compressible near-critical region. For instance, the partial molar volume of the solute at infinite dilution for naphthalene in ethylene at 12°C and 5.37 MPa was found to be equal to –15 200 cm^3/mol [32]. This very drastic volumic contraction is interpreted in terms of solvent structure and intermolecular forces. These intermolecular attractions are generally thought to occur when the solute size is larger than the solvent size, and when the characteristic energy for solute-solvent interactions is larger than the solvent-solvent interaction energy. Molecular dynamic simulations of both attractive and also repulsive mixtures have been reported [44]. In the case of an attractive mixture, the addition of solute disrupts the structure of the supercritical solvent and leads to the creation of regions in space near the solute molecules where the local density differs from the bulk density. A representative name used to describe this phenomenon of local density augmentation is "molecular charisma" [45]. This behavior is generally taken to describe specific short-range effects [41], which differ from the long-range correlations due to a critical behavior that leads to large partial molar properties in the vicinity of the critical point.

The solute partial molar volume can be expressed as a simple integral involving the direct correlation function [32]. Simulation and integral equation calculations have used simplified, spherical symmetric potentials (for example Lennard-Jones mixtures) to study supercritical systems [46]. The results represent ideals of molecular interactions which do not capture all of the structural and dynamics effects associated with the complex molecules in supercritical fluids. The "molecular charisma" is thought to be a dynamic exchange process with bulk molecule, at a frequency of about one of a picosecond [47], and may persist for 100 picoseconds [43]. The addition of a small amount of a volatile cosolvent to a supercritical fluid may dramatically increase the solute solubility. The solubility of salicylic acid in CO_2 at 55°C and 10 MPa is increased of 2 orders of magnitude by addition of 3.5% of methanol or acetone [48].

For highly dilute solute-cosolvent systems in a near critical solvent, theoretical arguments indicate that the enhanced solubility is due to solute-solvent and cosolvent-solvent interactions [49]. Cosolvent-solvent specific interactions, such as hydrogen bonding, charge transfer complex formation and dipole-dipole couplings appear to be important [50].

All the experimental studies have pointed out the occurrence of local density augmentation of a supercritical fluid around solute molecules. These experimental studies are based on the solubility of solids and on partial molar properties of dilute solutes in near-critical solvents [32, 40, 49, 51, 52] and also on spectroscopic techniques which provide information on solvation (short ranged interactions) and solvent structure [43, 45, 53, 54, 55, 56, 57, 58, 59].

Another approach of the solubility in supercritical fluid was derived from the association law and directly related to the fluid density [37]. In an ideal case, if one molecule of a solute A is associated with k molecules of a fluid B to form one molecule of a solvato complex AB_k in equilibrium with the system, we can express the equilibrium constant (K) as follows:

$$\begin{gathered} A + k\,B \rightleftharpoons AB_k \\ K = [AB_k] / ([A]\,[B]^k) \end{gathered} \tag{9}$$

$$\ln K + \ln [A] + k \ln [B] = \ln [AB^k] \tag{10}$$

where $[A]$ is the molar vapor concentration of the solute, $[B]$ is the molar concentration of the fluid, and $[AB_k]$ is the molar concentration of the solute in the fluid (usually $[A] << [AB_k]$). K can be expressed as $\ln K = \Delta H_{solv}/RT + q_s$, where ΔH_{solv} is the heat of solvation, and q_s is a constant. The concentration of the solute $[A]$ can be approximated by the Clapeyron-Clausius Equation: $\ln [A] = \Delta H_{vap}/RT + q_v$, where ΔH_{vap}

is the heat of vaporization of the solute, and q_v is a constant. Combining these expressions into 10, we get:

$$\Delta H/RT + q + k \ln [B] = \ln [AB_k] \quad (11)$$

where ΔH is the total reaction heat $\Delta H = \Delta H_{solv} + \Delta H_{vap}$ and $q = q_s + q_v$.

We can express the concentrations and the density of fluid (ρ) in g/l and thus $[AB_k] = C_2/(M_A + kM_B)$, $[B] = \rho/M_B$, where C_2 is the concentration of the solute in the fluid, and M_A and M_B are the molecular weights of the solute and the fluid, respectively. Then we get:

$$C_2 = \rho^k \exp((a/T) + b) \quad (12)$$

where $a = \Delta H/RT$ and $b = \ln (M_A + kM_B) + q - k\ln M_B$.

All the constants can be straightforward determined from experimental values and are reported in Table 5 for different solutes in CO_2 [37].

TABLE 5

Solubility constants in relation to Equation (12) for different compounds in CO_2 [37]

Compound	*k*	*a*	*b*
Steric acid	1.821	–10664.5	22.320
Oleic acid	7.922	–15360.5	-2.499
Behenic acid	1.935	–1201.8	-9.480
Tributyrin	9.566	–10219.1	-27.550
Tripalmitin	2.980	–2387.8	-12.150
Tristearin	9.750	–8771.6	-39.440
Triolein	5.216	–11386.5	2.415
Trilinolein	5.511	–10082.7	-4.060
Palmityl behenate	1.463	–2828.8	-1.251
Behenyl behenate	3.250	–7328.1	0.824
α-tocopherol	8.231	–17353.5	0.646
Cholesterol	12.095	–9460.0	-50.488
Water	1.549	–2826.4	-0.807
Caestol	7.202	–3820.3	-37.022

It is not expected that the constant *k* will be an integer. The association constant *k* expresses an average equilibrium association number, which is a characteristic constant for given fluid and solute. As classically observed the solubility is more directly related to the density than to the pressure of the fluid.

Equation (12) was demonstrated to be valid for many solute solubilities and for solute concentrations (C_2) lower than 100-200 g/l, since then the density of the solution is usually not very different from that of the pure fluid under the same conditions.

Whatever the solubility description, it is never necessary to know the equations of state and the equilibrium data corresponding to the pure fluids or mixtures. It is not the subject of this paper to develop the different types of equations of state, but these equations will have a central role in supercritical fluids, because it is necessary for process design to predict equilibrium and transport properties. Fluid phase equilibria and critical data are also essential to process design. Binary [60] and ternary mixtures have been reasonably well studied, and correlated data are available in case of some of the more prevalent modifiers. For example, the phase diagrams of methane-heavy hydrocarbon mixtures measured using an infrared absorption method are used to estimate new interaction parameters for the Peng-Robinson Equation [39].

1.2.2 Solubility behavior in pure water

Fluids and mixtures can present specific behavior such as the relative static permittivity (ε_r) evolution of pure water (Table 4). ε_r variations show that water becomes a good organic solvent in supercritical region. Under ambient conditions, liquid water has a high ε_r (e.g. 80), which arises from dipoles of individual molecules and association of molecules due to hydrogen bondings. Under supercritical conditions, much of these intermolecular associations break down [61] and [62] causing the dielectric constant falling down. For example, benzene shows a complete miscibility in supercritical water, whereas in liquid water under ambient conditions the benzene solubility is equal to a few ppm [63]. On the contrary, salt solubility falls down by some orders of magnitude as the density falls down by 3. For example, the NaCl solubility (in weight percent) is equal to 26.4 in liquid water (at ambient conditions) and only to $1.5\ 10^{-4}$ in supercritical water [64].

This behavior can be a drawback in processes for the oxidation of wastes, as it causes a deposition or/and corrosion of the reactor. However, the Modell's patent claims the exploitation of the salt precipitation for a desalinator at conditions just above the critical point of water. The solubility of many inorganic salts is

negligible and induces their precipitation from a feedstock such as brine [65]. After this general presentation of critical and supercritical behavior of fluids, we would like to point out the possibility of tuning fluid characteristics from liquid to gas without any discontinuity. Indeed, each reaction which is possible in liquid or gas is possible in supercritical fluid. Moreover, supercritical fluid processes can continuously use the properties of liquid, supercritical fluid (which are specific) and gas. For extraction, it is possible during the process to realize liquid-liquid extraction then supercritical fluid extraction and stripping (Fig. 5) as used in the ROSE process [66].

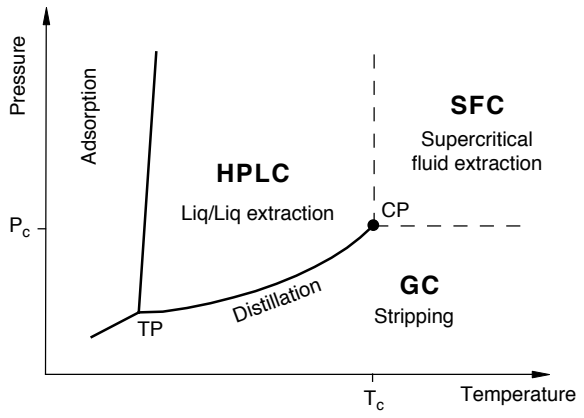

Figure 5

Schematic representation of extraction types as a function of location in *PT* diagram. HPLC, GC, SCF are high pressure liquid chromatography, gas chromatography and supercritical fluid chromatography, respectively.

2 CHEMICAL REACTIVITY

2.1 General aspects

The interpretation of reaction rates by transition state theory, involving thermodynamic treatment of activation parameters, implies the concept of an activation volume [67]. This approach is the thermodynamic framework which allows the interpretation, the correlation and the prediction of rates of chemical reactions and so creates a bridge between thermodynamics and kinetics.

This theory views a chemical reaction as occurring via a transition state species or an activated complex noted M^*. The transition state is the state of maximum energy along the reaction coordinate pathway, where this pathway between the reactants and products corresponds to the minimum energy on the potential energy surface.

Transition state theory pictures a reaction between A and B as proceeding through the formation of an activated complex M^* that falls apart by unimolecular decay into product P:

$$A + B \rightleftharpoons M^* \rightarrow P$$

Starting from M^*, the P formation occurs with a rate equal to k_2^* $[M^*]$, where k_2^* is the rate constant expressed in s^{-1}. The concentration of activated complex is in strict thermodynamic equilibrium with the original reactant:

$$[M^*] = K^* [A] [B] (\gamma_A \gamma_B / \gamma_M^*) \quad (13)$$

where K^* is the concentration based equilibrium (in $l \cdot mol^{-1}$), $[A]$ and $[B]$ are the molar concentration of A and B reactants, respectively.

The global reaction rate can be expressed as:

$$\text{Rate} = k_o (\gamma_A \gamma_B / \gamma_M^*) [A] [B] = k [A] [B] \quad (14)$$

with k is the global rate constant expressed in $l \cdot mol^{-1} \cdot s^{-1}$, k_0 is the rate constant in the ideal reference system ($\gamma_A = \gamma_B = \gamma_M^* = 1$) and the $\gamma's$ are the activity coefficients in the mixture [67] and [68].

If the vibration-like motion along the reaction coordinate occurs with the same frequency as the complex approaches the transition state, k_0 can be expressed with the Eyring Equation as:

$$k_0 = \alpha (k_B T/h) K^* \quad (15)$$

α is the transmission coefficient, or the probability that the decomposition of the transition state falls into product P, which is usually equal to unity. k_B is the Boltzman's constant, h is the Planck's constant, T is expressed in Kelvin [67]. The equilibrium constant K^* is related to the standard variation of Gibbs energy by the classical equations:

$$\Delta G^* = -RT \ln K^* \quad \text{and} \quad (\partial \Delta G^*/\partial P)_T = \Delta V^* \quad (16)$$

The pressure derivative of activation energy gives the activation volume ΔV^* of activated complex.

It is equivalent to differentiate the rate constant k, which must be expressed in pressure independent unit as a function of k_X, which is expressed in mole fraction (or molality), by the following relation:

$$k\, C_T = k_X \qquad (17)$$

where C_T is the total concentration.

Then the derivative of the global rate constant yields to:

$$(\partial \ln k/\partial P)_T = (\partial \ln k_X/\partial P)_T - (\partial \ln C_T/\partial P)_T \qquad (18)$$

$$(\partial \ln k/\partial P)_T = -\Delta V^*/RT - K_T \qquad (19)$$

This last equation can be generalized:

$$(\partial \ln k/\partial P)_T = -\Delta V^*/RT + \beta K_T \qquad (20)$$

where β is the number of products minus the number of reactants.

Similar results can be obtained from the fundamental thermodynamic equations that describe the pressure dependence of the chemical potential μ_i of a solute i in an ideal solution:

$$(\partial \mu_i/\partial P)_T = V_i \quad \text{and} \quad \mu_i = \mu_{i0}(C) + RT \ln C_i \gamma_i \qquad (21)$$

where C_i is expressed in molarity [69].

In Equations (19) and (20), the activation volume is defined as $\Delta V^* = V_M - V_A - V_B$, where V_i is the partial molar volume of the i species.

ΔV^* provides a valuable mechanistic information about the transition state that complements which can be added to the activation enthalpy and entropy information.

For the classical incompressible liquid used in high pressure chemistry, the term βK_T in Equation (20) is negligible and the magnitude of the intrinsic activation volume is typically between –50 and 30 $cm^3 \cdot mol^{-1}$ [69]. In these conditions, Table 6 shows the evolution of the rate constant (k/k_0) as a function of ΔV^* and P, with all parameters assumed to remain constant for this demonstration. It is worth noting that at working pressure used in supercritical fluids, generally in the range from 1 to 50 MPa, the pressure effect on the rate constant (k/k_0) is unimportant.

TABLE 6

Pressure effect on the rate coefficient (k/k_0) as a function on ΔV^* at 60°C for an incompressible fluid

ΔV^*	k/k_0				
$cm^3 \cdot mol^{-1}$	10 MPa	50 MPa	100 MPa	500 MPa	1000 MPa
–50	1.12	2.47	6.1	8386	$70.3\ 10^6$
–30	1.11	1.72	2.96	226	51127
–15	1.06	1.31	1.72	15	226
+15	0.95	0.76	0.58	0.06	$4\ 10^{-3}$
+30	0.90	0.58	0.34	$4.4\ 10^{-3}$	$2\ 10^{-5}$

However it is well known that in a pressure range from P_C to 3 P_C the rate constant k_X changes significantly of a three orders of magnitude, as schematically shown in Figure 6.

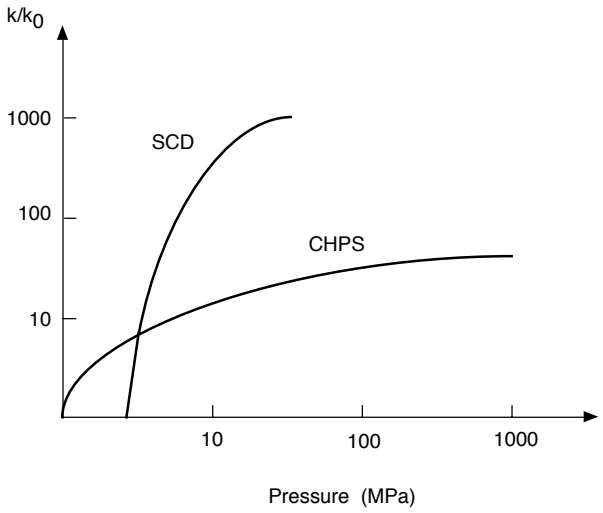

Figure 6

Schematic representation of pressure effect on global rate constant in supercritical domains (SCD) and classical high pressure synthesis (CHPS).

This change (expressed as a function of reduced pressure) is gradual and similar for chlorotrifluoroethane dimerization [70], hydrogen iodide decomposition [71] or Menschutkin reaction of triethylamine and ethyl iodide [72].

These effects are not limited to the dilute concentration region and they are not specific to a

particular class of bimolecular reactions since the expected transition states of the three previous reactions are different [73]. So the unusual pressure effect on reaction rates in a supercritical fluid solvent indicates that the solvent properties are extremely pressure sensitive. Unusual large activation volumes ($|\Delta V^*| > 10^3$ $cm^3.mol^{-1}$) have been reported for reactions in supercritical fluids which account not only for the direct effect of pressure but also for the variation of solvent properties with pressure [70, 74, 75, 76].

Generally the apparent activation volume is not a constant, it can vary with both pressure and temperature [69] and [74]. The activation volume can be separated in two terms [69]. The first contribution (ΔV^*_{intr}) accounts for volume changes arising from modifications in bond lengths and angles during the formation of the products. (ΔV^*_{intr}) is mainly the "mechanical" effect of pressure on the rate constant. The second contribution accounts for solvation which includes the effects of pressure on diffusion (ΔV^*_{diff}), the electrostatic interactions (ΔV^*_{elec}), the compressibility of the fluid phase ($\Delta V^*_{comp} = \beta K_T$) and the phase behavior (ΔV^*_p) [77].

Concerning the specific aspects of phase equilibrium behavior of system involving supercritical fluid which is very important for industrial application, it is worth noting that supercritical fluid solvent properties can be modulated smoothly and continuously by changing pressure and temperature. As an exemple, we consider the hydrothermal oxidation of organic compound by oxygen addition for three operating conditions [10]. The first condition at 300°C and 8.5 MPa leads to a residence time of one hour and a destruction efficiency of 90% in weight.

The second condition at 300°C and 25 MPa leads to a residence time of one minute and a destruction efficiency of 95% and the third condition at 500°C and 25 MPa leads to a residence time of 10 seconds and a destruction efficiency of 99.9%. The influence of the phase behavior between the first and second conditions is only due to oxygen solubility in the dense phase which is very large at 300°C and 25 MPa (higher than the stoichiometry) and very low (10^{-3} g/g) at 300°C and 8.5 MPa. The decrease of the resident time and the increase of the efficiency between the second and the third condition is due to the temperature increase as classically shown by the Arrhenius Equation. The influence of phase equilibrium on the kinetics of reactions induces very different reactor design. For an industrial site which treats 1 m^3 per hour of sludge, the reactional volume is 1 m^3 for the first conditions, and 25 l for the second or third operating conditions. The associated investment cost is also much lower for the two last conditions.

The different types of reactions will be no more developed and the kinetic and diffusion control studies are not presented in regard of the rich literature related to these fields [9, 68, 69, 78, 79].

Another important research field concerns the inorganic reactions. Many studies have been reported such as solvent and ligand exchange reactions, ligand substitution reactions, isomerization reactions, addition and elimination reactions, electron transfer reactions, photochemical and processes, bioinorganic reactions [80]. We limit the presentation of inorganic reactions to the pressure effect on the solvent and ligand exchange reactions. Figure 7 exhibits all solvent exchange mechanisms and the associated pressure effects.

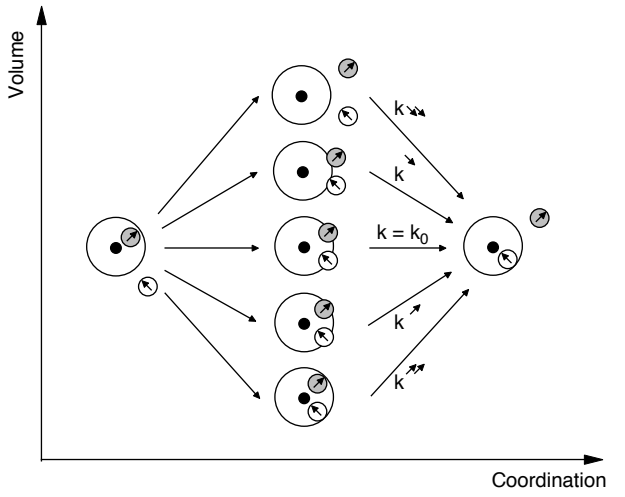

Figure 7

Schematic representation of the transition state at crucial points in the spectrum of solvent-exchange mechanisms (adapted from [69]).

More generally, the extreme negative values of the activation volume are related to the rapid change of the fluid density with pressure or temperature and as a consequence the rate constant is rapidly increasing from gas-like to liquid-like value. This rate constant evolution is not an indication of important effects on

reaction behavior due to the proximity of the critical point. The interest of supercritical fluid as medium for chemical reaction is located in product control such as mass, separation and stereoregulation control. Moreover, phase equilibrium in supercritical fluid can be tuned smoothly and continuously by changing pressure or temperature and can significantly modify the reaction behavior. After discussing general aspects of chemical reactivity in supercritical fluids, polymer synthesis applications and hydrothermal waste treatment are successively presented.

2.2 Polymer synthesis applications

A supercritical fluid offers a potential such as polymerization medium where it can be used as a solvent, a monomer or both. In general the polymer formation by addition polymerization of unsatured monomers is followed by a decrease of the activation volume, and therefore is enhanced by an increase in pressure. To understand the polymerization mechanisms in supercritical fluids and the effects of the pressure, it is necessary to develop the rate equations of the different reactions involved in a free-radical polymerization (rate of radical formation, of initiation, propagation, termination and chain transfer). From a general point of view, high pressures induce large rates of propagation and degrees of polymerization, an elevation of ceiling temperatures, and also variations in polymer tacticity and structure.

The pressure increase induces the polymer formation but stops the termination reaction and therefore leads to high molecular weight. This is rationalized in terms of the activation volume concept. The temperature increase involves the inverse effect and then a polymolecularity rise. Indeed the great number of free radical formation, involved by the temperature rising, grows up the chain transfer and so the number of initiated chains. We present hereafter different polymerization types performed in supercritical media.

2.2.1 Polyethylene synthesis

The first supercritical polymerization reaction was discovered in 1933 at *Imperial Chemical Industries*. The reaction of benzaldehyde with ethylene at 170°C and at 140 MPa produced a “waxy white solid” later recognized as a polyethylene. Since that time, the supercritical method is still used to produce ethylene polymers.

Ethylene oligomers are synthesized by reacting ethylene and a Ziegler type catalyst (such as triethylaluminium). The polymerization is performed in a single step at a pressure varying from 136 to about 272 MPa and at a temperature from 176 to 287°C using catalyst concentrations from 10^{-4} to 10^{-2} M. The reaction leads to a conversion from 30 to 90 weight% for a residence time of 5 minutes or longer [81].

High molecular weight products from ethylene in presence of peroxygen type catalyst were performed at high pressure and temperature [82]. At low temperature (100°C) and in a range of pressure from 340 to 680 MPa, the obtained polyethylene is without any branching with a density as high as 0.970. For a temperature from 150 to 325°C and a pressure from 102 to 272 MPa, the polymer product contains both long and short-chain branching with densities from 0.915 to 0.935. In fact, the short-chain branching due to the specific intramolecular hydrogen-transfer reaction producing ethyl side chains, has been found to be directly proportional to temperature and inversely proportional to pressure.

The pressure effect is explained by the different activation volume for the branching and propagation step. Supercritical ethylene can also be copolymerized with a wide variety of monomers such as acrylates, vinyl alkyl ethers, dienes and sulfur dioxide.

2.2.2 Polystyrene synthesis

Polymerization of styrene was studied in supercritical alkanes with several solvent/initiator systems [83]. The synthesis is performed at a pressure from 6.9 to 34.5 MPa and at a temperature from 160 to 180°C, during 1 to 9 hours, in a batch or in a flow reactor with a continuous monomer alimentation. The butane/*t*-butyl peroxide system was tested. In the case of a batch reactor, it leads to a polydispersity between 2.2 and 2.4, the number and weight average molar weights ranging from 3 900 to 8 700 and from 9 500 to 18 300 $g{\cdot}mol^{-1}$ respectively, with an efficiency from 9 to 20%. Polymer chains grow and quickly reach their final size. As soon as they precipitate in the supercritical phase, the propagation reaction cannot be carried out.

The chromatography pattern shows an unimodal distribution. In the flow reactor, the monomer concentration is kept constant during the polymerization reaction. The polymer is recovered at about 1 hour intervals. The distribution obtained

is unimodal and with a polymolarity around of 1.7. At 17.2 MPa and 160°C, this process allows to reach higher molecular weight fractions with lower polymolecularities.

2.2.3 Polymerization reactions in supercritical CO_2

Classical polymerization methods use large volumes of organic solvents which must be recovered and recycled. Environmental considerations drives on use of CO_2 like solvent. Indeed CO_2 is a nontoxic, nonflammable, inexpensive solvent and it is unreactive in many polymerization processes. Morever its critical point is low.

The range of polymers which can be synthesized homogeneously in CO_2 is limited since only amorphous fluoropolymers and polysiloxanes show an appreciable solubility in CO_2. However it is possible to perform dispersion polymerizations in supercritical CO_2 where a CO_2- soluble polymeric stabilizer is used to stabilize a CO_2- insoluble polymer as a colloid. The successful stabilization of the polymer colloid during polymerization results in the formation of high molar mass polymers with high rates of polymerization. This methodology allows to synthesize polymers such as poly(methylmethacrylate) [84].

2.2.4 Free radical polymerizations

Synthesis of high molar mass fluoropolymers using homogeneous free radical polymerization methods was performed in supercritical CO_2. 1,1-dihydroperfluorooctyl acrylate (FOA) and azobisisobutyronitrile (AIBN) are mixed, heated at 59°C and pressurized at 70 MPa during 1 hour and then put at 207 MPa. The polymerization is carried out in these conditions during 48 hours. At the end of polymerization, CO_2 is vented and the non-soluble polymer in CO_2 at lower pressure is precipitated. In supercritical conditions, the radical diffusion into the bulk solvent is easy because of the low viscosity of CO_2. A rate of AIBN decomposition is observed 2.5 times as low as the rate found in benzene at ambiant pressure (this because of higher dielectric strengh of benzene). The molecular weight of polymer recovered is around 270 000 $g.mol^{-1}$. Copolymers of fluorinated monomers with conventional hydrocarbon-based monomers (such as methyl methacrylate, butylacrylate, styrene, ethylene) can be made under similar conditions [85]. Preparation of a thermoplastic resin or resins under supercritical conditions was also performed [86].

2.2.5 Polycondensation reactions

In order to decrease the reaction temperature, supercritical CO_2 was used as solvent for the formation of polyesters from diacid chlorides and diols. Higher degrees of polymerization were observed when fluorinated diols were used. Indeed, the resulting polyesters were partially fluorinated and therefore presented higher solubilities in CO_2. But in general, molecular weight and degree of polymerization are limited by the oligomer precipitation at a relatively early stage of the reaction. To avoid this problem and to improve molecular weight, polymeric stabilizers such as fluoroether surfactants are used [87].

Production of polyesters was also performed by using enzymes and supercritical fluids [88]. The polycondensation is performed by reacting an organic diol with either an organic diester or an organic dicarboxylic acid in the presence of supercritical CO_2 and solid esterase (preferably a lipase) enzyme, at a temperature from 20 to 80°C and a pressure from 69 to 345 MPa, in a batch reactor during 120 hours. So the esters produced herein contain from 3 to 50 repeating ester units and have a polydispersity index between 1.0 and 4.0. The ring-opening metathesis polymerization of bicyclo (2,2,1) hept-2-ene (norbornene) in supercritical CO_2 and CO_2/methanol mixtures using a $Ru(H_2O)_6(tos)_2$ initiator: CO_2 was found as a viable medium for this type of polymerizations with no incorporation in the polymer structure [89]. The second further important development of supercritical fluids as reactive media concerns the waste treatment.

2.3 Hydrothermal waste treatment

Industrial and municipal wastewaters are destroyed by specific treatments (physico-chemical, biochemical, etc.). After sludge volume reduction, the resulting products are incinerated and/or buried in the dumping ground or landfilled. Incomplete destruction of pollutants should become a dramatic problem for environmental protection in the further years. The environmental regulation evolution and the increasing wastewater disposal cost lead to a new concept of complete destruction of toxic substances and sludges. Thus, alternative techniques limiting the risk of

secondary pollution are developed (thermolysis, plasma vitrification, wet air oxidation, supercritical water oxidation, etc.). During the past decade, mainly in United States, a number of universities and companies have investigated the wastes destruction in hydrothermal media [9] and [90] (oxidation in sub- and supercritical water, T_c = 374°C and P_c = 22.1 MPa). The purpose is twofold: final volume reduction of wastes and obtention of non toxic end products. The reactivity of such a medium is related to: i) the low viscosity; ii) the high diffusivity; iii) the monophasic fluid phase which suppresses transport phenomena at the interfaces in multiphasic systems, and iv) the ability of supercritical water (nonpolar solvent behavior) to dissolve oxygen and organic compounds. More recently, these new technologies have been also developed to achieve industrial applications.

We will first present results concerning model molecules destruction using near-critical and supercritical water. The influence of various parameters governing the transformation (pressure, temperature, residence time, additive) will be investigated. Then, we will present the results concerning real waste treatment: biological and industrial wastewaters or sludges, and military wastes.

2.3.1 Model compounds

Oxidation of wastes in supercritical water has been introduced by M. Modell in the early 1980's [65]. He has investigated several organic compounds by supercritical water oxidation (SCWO) [91], and found conversion rates greater than 99.9%, even for polychlorobiphenyl (PCB) which are decomposed without any dioxins formation. Many chemical compounds have been successfully treated by SCWO with high destruction efficiencies [64]. Inorganic compounds were also present in the bench-scale tests and the process was successfully operated even if they were not destroyed. Residence times are smaller than 1 min in supercritical processes in comparison with one hour in subcritical ones, like Zimpro [92]. But for subcritical temperatures and higher pressures (typical value of SCWO), residence times could be considerably reduced (in the order of a few minutes) and good efficiencies could be reached as the further examples will show it.

Reaction pathways lead to non toxic gaseous products in hydrothermal conversion (no NO_x, SO_2, HCl). Several teams have worked on kinetics and degradation mechanisms, for specific reactions with model compounds. Many model molecules have been studied, such as carbon monoxide, methanol, ethanol and ammonia [93, 94, 95], p-chlorophenol [96], acetic acid and 2,4 dichlorophenol [97], phenol [98] and sugars and cellulose [94, 99, 100]. The organic and oxidant orders of the global reaction and the activation energy have been determined.

Methanol as a high refractory compound for oxidation and glucose as a model of the wet cellulose wastes are generally used for the working validation of the pilot efficiency. Figure 8 shows the influence of the reaction temperature on the reaction efficiency, in terms of Chemical Oxygen Demand (COD) or Total Organic Carbon (TOC) reduction in the liquid phase for methanol and glucose and for phenol.The results will be discussed now.

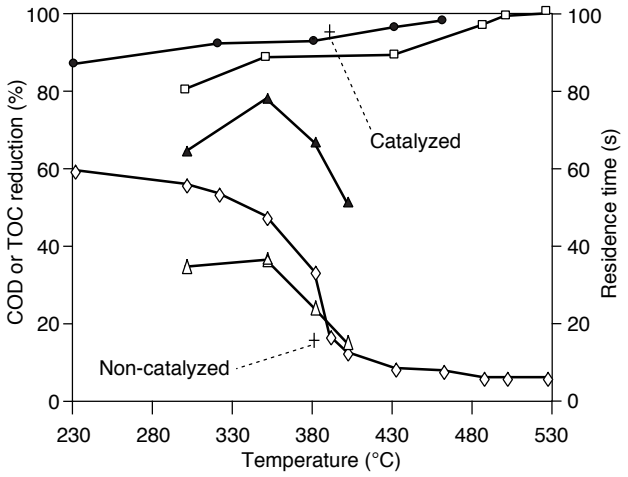

Figure 8

Evolution of hydrothermal oxidation of model compounds in near critical and supercritical water at 26 ± 2 MPa in a plug flow reactor.

COD reduction: ● glucose [108], □ methanol [108], H_2O_2 as oxidant; TOC reduction: Δ phenol [103], + phenol [102], O_2 as oxidant; conversion rate: ▲ phenol [103], O_2 as oxidant; ◊: residence time in s.

It must be underlined that for all experiments reported on Figure 8, the evolution of the residence time (t_s) in the plug-flow reactor during the conversion of those model compounds is based on the density of the phase in the reactor. It means that for all

temperatures, this residence time corresponds to the same value of the reactor volume and to the same flow-rate of the treated effluent.

We note that subcritical region does not lead to a complete conversion for those compounds, and we also evidence a constant behavior of the reaction efficiency around the critical point. Results obtained above 530°C with t_s = 6 s for methanol, which give COD reduction of 99.95% and no CO product, are different from those of J.W. Tester [101] which led to 40% of CO for a conversion rate of 96% in their experimental conditions. They propose the CO oxidation in CO_2 as a limiting step for the methanol oxidation by oxygen at high temperature. The use of the hydrogen peroxide which as injected at 20°C into the reactor in the first case can be explain this different results.

The methanol oxidation rate constant can be expressed in the Arrhenius form by $k = A \exp(-E_a/RT)$, as shown in Table 7, where E_a is the activation energy and A is the preexponential factor.

TABLE 7

Global kinetic for methanol oxidation in sub- and supercritical water at 25 MPa, assuming a first order reaction

Oxidant and injection temperature (°C)	Activation energy E_a (kJ/mol)	Preexponential factor (A) (s^{-1})	Temperature range (°C)	References
O_2 (400°C)	409	$10^{26.5}$	450 - 550	[101]
H_2O_2 (400°C)	115	10^7	450 - 550	[95]
H_2O_2 (20°C)	58	4860	300 - 530	[94]

When hydrogen peroxide is injected into the reactor at 20°C, we evidence that H_2O_2 is a better oxidant than oxygen, as previousely published [97], and when the degradation of H_2O_2 takes place into the reactor, conversion rates are higher at the same temperature. The mechanism of organic molecule degradation by hydrogen peroxide seems to have an initiation step in which OH radicals are generated, and contribute to decrease the activation energy of the global reaction.

Pyrolytic gasification of glucose was performed in supercritical water [99]. Complete gasification was obtained for glucose concentrations lower than 0.1 M at 600°C and 34 MPa for t_s = 30 s. Major products formed in the liquid phase and in the gas phase were identified in hydrolysis as in oxidation [100]. With the use of an oxidant, at only 470°C and 25 MPa for t_s = 8 s and for the same concentration range, the COD reduction is of 99.5% with no CO product [94]. Figure 8 also presents results obtained for the phenol oxidation by oxygen in excess, in an isothermal plug flow fixed-bed reactor in the presence of a solid catalyst (12.1% weight of copper oxide and 22.7% of zinc oxide, supported by a steam-treated porous cement) [102]. In this case, phenol is oxidized to carbon dioxide at much lower temperature, and the removal efficiency of the reaction is enhanced by a factor greater than 4. Similar experiments have been investigated without any catalyst [103], and are drawn in terms of TOC reduction and conversion rate of phenol. The conversion of organic carbon to CO_2 is always lower than the conversion of phenol, which indicates that products of incomplete oxidation are present [104]. During the uncatalyzed process, many different carboxylic acids are formed. In the catalyzed process, the reactions leading to the opening of the aromatic ring are very fast and only acetic and formic acids are observed [105]. Moreover, the production of carbon monoxide known in uncatalyzed oxidation is not enhanced by the presence of a catalyst.

2.3.2 Industrial wastes

Eco Waste Technologies obtained good results on several excess hazardous materials [106] as paint sludge, greases and lubricants, waste oil, mixed solvents, where conversion rates are always higher than 99.9%. For sludges (municipal, refinery, paper mill and chemical industry), we note the same removal efficiency regarding TOC or COD reduction, and Total Solids (TS) removal efficiencies are between 50 and 70% for all those sludges, which could be attributed to the mineral fraction of the sludge.

Paper mill sludges containing organic and mineral compounds have been treated [107]. At 600°C and 25.5 MPa, t_s = 10 to 600 s, destruction efficiencies are between 80 and 90% regarding Total Solid (TS) decrease (for an initial TS concentration of about 40 000 ppm), and TOC and Total Organic Halogen (TOX) removal efficiencies are greater than 99%.

Deink sludges from paper industry have been treated with hydrogen peroxide as oxidant [108]. Initial Chemical Oxygen Demand (COD) for those effluents is about 10 g/l and salt concentrations are about 600 ppm. As shown in Figure 9, at 500°C and 28 MPa, we note a reduction of 99% of COD for deink sludges with low total solid concentration. However, for higher total

solids concentration (TS = 17 g/l), higher residence times or higher reaction temperatures seem to be necessary to achieve complete reaction.

Similar experiments have been achieved on the same effluents [109] and are reported on Figure 9.

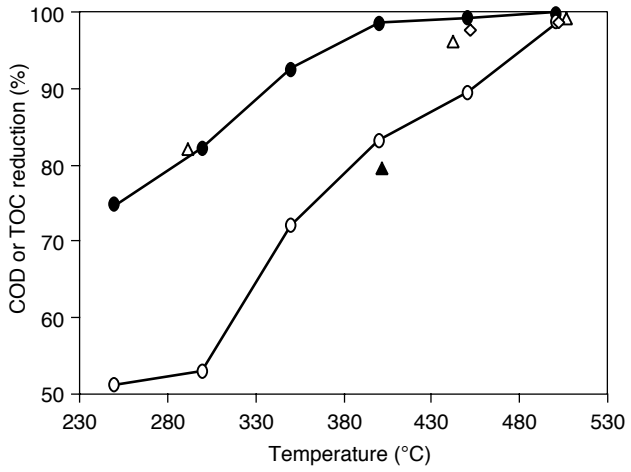

Figure 9

Influence of solids concentration on near critical and supercritical water oxidation of industrial wastes at 26 ± 2 MPa (t_s = 1 min, O_2 or H_2O_2 in excess). ●: DNT without sludge [110]; O: DNT-sludges (30 000 ppm of solids) [110]; Δ: deink sludges (600 ppm of solid particles) [108]; ▲: deink sludges (17 000 ppm of solid particles) [108]; ◊: paper mill sludges [109].

Wastewaters with 0.2 weight% of phenol compounds (TOC = 1840 ppm) are studied in regard to the addition of 3 weight% of biological sludges (COD = 39 g/l) [110]. TOC removal efficiencies are independent of residence times in supercritical area.

Table 8 shows this influence in subcritical area with the reaction temperature. We see that quite complete conversion could be possible for 350°C and a residence time of 7 min with oxygen as oxidant.

Moreover, with 3% sludge solids, at 300°C and 240 s residence time, the COD removal efficiency decreases from 87.4% to 68.5% for pressures of 27.6 MPa and 13.8 MPa, respectively.

In the last case, the oxygen dissolution rate is a limiting factor and the sludge solid concentration seems also to affect the global conversion rate of the reaction.

TABLE 8

COD decrease during subcritical oxidation of DNT wastewaters by oxygen at 27.6 MPa, as a function of reaction temperature and residence time [110]

Residence time (s)	Temperature (°C)		
	250	300	350
60	74.9	82.2	92.5
240	78.5	89.7	95.7
420	74.9	91.5	99.6

The previous table shows that some industrial wastes could be entirely converted at subcritical temperatures, if the pressure is high enough to provide a good dissolution of oxygen in the medium.

Concerning residence times to achieve this goal, one must keep in mind that the density at 350°C is seven times as great as the typical density of supercritical aqueous media, so that the reactor volume is the same as in supercritical water oxidation if residence times are in the minute order, and this for the same capacity of treatment.

The solid concentration influences the conversion as shown in Figure 9 for DNT (dinitrotoluene) wastewaters and deink sludges. The batch test results demonstrate that the oxidation rate of the DNT waste and sludge in the supercritical region is comparable to DNT without any sludge solids for temperatures greater than 450°C and residence time longer than to 4 min. At lower temperatures, the presence of the sludge solids seems to slow the oxidation rate for 1 min as residence time.

We observe the same phenomena for deink sludges [108]. Some tests were also conducted using continuous-flow reactor for DNT wastes with sludge solids, and COD removal efficiencies greater than 99.7% were obtained for 400 and 450°C, with residence time respectively of 60 and 15 s, with acid pH. Acid medium seems to lead to better destruction, with abstraction of corrosion problems, in comparison with experiments after neutralization, as pointed on Figure 9.

2.3.3 Biological and biopharmaceutical wastes

Figure 10 illustrates the destruction of excess activated sludge as well as the production and transformation of acetic acid at temperatures ranging from 300°C to 450°C, for biological sludge containing

4.2% solids with a COD value of 52 g/l [111] and sludges containing 5% solids with COD value of 46.5 g/l [112].

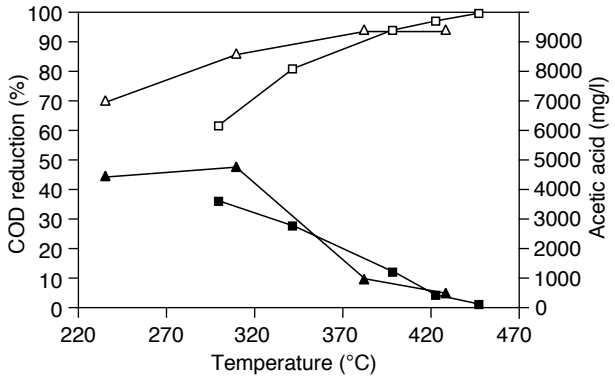

Figure 10

Oxidation of biological sludge in sub and supercritical water by excess of oxygen with respect to COD. Δ: COD reduction for t_s = 60 min [111]; □: COD reduction for t_s = 5 min [112]; ▲: acetic acid production for t_s = 60 min [111]; ■: acetic acid production for t_s = 5 min [112].

Quite complete destruction is obtained for temperatures between 450 and 500°C, and produced ammonia needs a higher temperature to be completely converted [113].

Acetic acid is often found in effluents from wet air oxidation, subcritical water oxidation and anaerobic digestion processes. In all tests involving subcritical temperature conditions (and pressure corresponding to the state saturation, e.g., 8.2 MPa at 300°C), considerable amounts of acetic acid are formed, as shown on Figure 10.

At supercritical conditions, the produced acetic acid is rapidly oxidized and quite complete destructions are achieved.

Pharmaceutical and biopharmaceutical products [109] and [114] have been successfully treated and a conversion rate of 97% at 550°C for pharmaceutical wastewaters of 20 000 ppm for initial TOC was found. But, in this last case, the operating system is limited by plugging because of the high salt concentration (3 weight%).

2.3.4 Military wastes

Oxidation chemistry of energetic materials as explosives and pyrotechnics (PEPs) in supercritical water have been studied [115]. Large amounts of NO_x are produced in the conventional combustion chemistry of PEPs. The SCWO of several explosive compounds (ammonium perchlorate, cyclotrimethylene trinitramine, nitroguanidine, 2,4,6-trinitrotoluene, etc.) leads to destruction efficiencies greater than 99% at 600°C and 37 MPa, with an excess of hydrogen peroxide and a residence time of 11 seconds.

Conditions of complete oxidation for hydrocarbon elements have been well established, but the nitrogen chemistry of energetics is more complicated and the nitrogen is always distributed among a group of products like N_2, N_2O, NO_2^- and NO_3^-, where N_2 represents the major compound.

American Government sponsored programs for Department of Defense hazardous wastes, solid propellants and chemical agents. In *General Atomics* [116], the influence of using catalysts, additives and alternative oxidants on conversion rates is studied to identify processing conditions which could increase reaction rates at lower temperatures.

At high temperature, e.g. 550°C, the conversion of organic compounds rapidly occur, but this temperature is necessary to destroy intermediates species, for example, methanol and methylphosphonic acid in the case of the degradation of dimethylmethylphosphonate (DMMP).

Results obtained on industrial wastes show that hydrothermal oxidation appears to be a competitive process for aqueous waste treatment. At last, it is worth noting that the hydrothermal oxidation of wastes is free of toxic end products and reduces final volume of wastes. The process optimization will be reached by the identification of intermediate species and by a better knowledge of reaction pathways and energy balance.

3 POLYMER PROCESSING

Polymeric materials may be expected to show a wide range of interactions with a supercritical fluid, varying from quite no effect to very pronounced effects based upon dissolution or even degradation of them. The potential interactions between a polymeric material and a supercritical fluid, and possible applications are outlined in Figure 11.

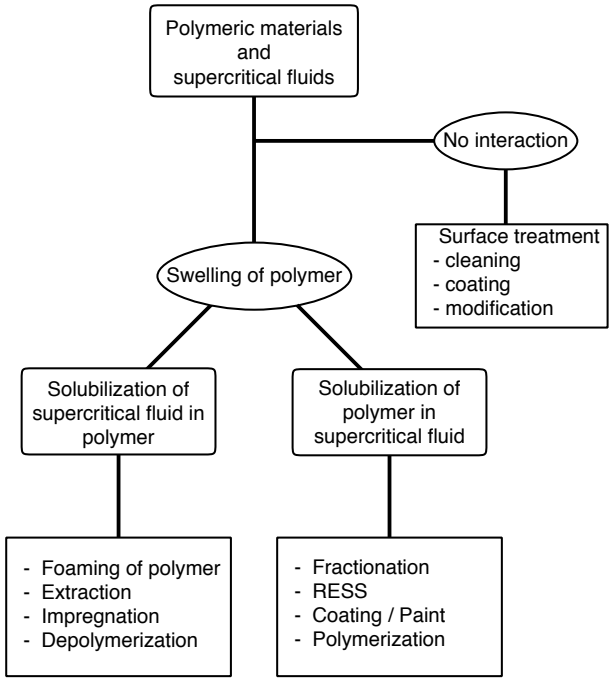

Figure 11

Schematic CO_2-polymer interactions and potential applications.

In this presentation, the changes in mechanical and surface properties when polymeric materials do not interact with the fluid are not developed. The swelling of polymeric materials which requires a knowledge of the interactions of polymers with the fluid is discussed in details. In the following section, after a general review of thermodynamic aspects of polymer-fluid interactions, we will therefore focus on polymer fractionation, impregnation and depolymerization.

3.1 General aspects

3.1.1 Solubility criteria

The thermodynamic criteria for the solubility of a polymer in a solvent are defined by the following equations:

$$\Delta G_m = \Delta H_m - T\Delta S_m < 0 \text{ and } (\partial^2 \Delta G_m/\partial \varphi^2)_{T,P} > 0 \quad (22)$$

where ΔG_m, ΔH_m, ΔS_m are the free energy, the enthalpy and the entropy of mixing respectively and φ is the volume fraction of polymer.

Three forms for the Gibbs free energy function are possible for binary systems corresponding to the three cases of immiscibility, partial miscibility, and complete miscibility as shown in Figure 12.

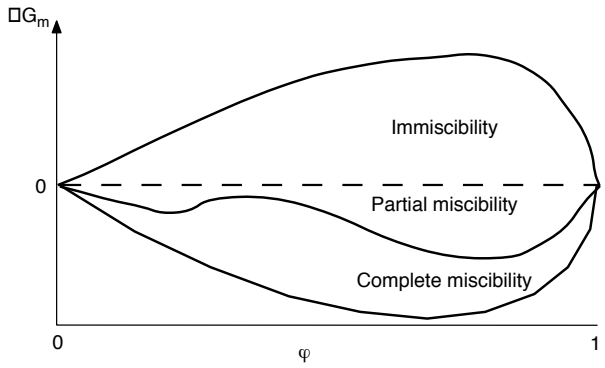

Figure 12

Schematic Gibbs free energy of a mixture with respect to the polymer concentration.

These different forms of the Gibbs free energy represent the behavior of a polymer in different solvent systems, or the behavior of a polymer in a given solvent but at different temperatures or at different pressures.

In partially miscible systems, ΔG_m is negative and, it shows an upward peak in the composition range from φ_1^b to φ_2^b defined by the co-tangential points (Fig. 13).

In this region, the solution will separate into two phases in equilibrium, which have the same chemical potential. The first phase, with a composition φ_1^b corresponds to a fluid rich phase or polymer-lean phase and the second phase, with a composition φ_2^b, corresponds to a polymer rich phase.

These compositions, with an exposant *b*, represent the binodal points. In the composition range from φ_1^s to φ_2^s, the second derivative of the Gibbs free energy of the mixture is negative and so the solution is unstable and undergoes a spontaneous phase separation, known as spinodal decomposition. For a binary system, the spinodal curve is defined by $(\partial^2 \Delta G_m/\partial \varphi^2)_{T,P} = 0$, and the thermodynamic condition of instability resulting in spinodal decomposition is that this derivative is negative. The composition ranges from φ_1^b to φ_1^s and from φ_2^s to φ_2^b represent the metastable regions. In these regions, we can consider that there is a barrier for the initiation of nucleation, but once the new phase is formed it grows very rapidly.

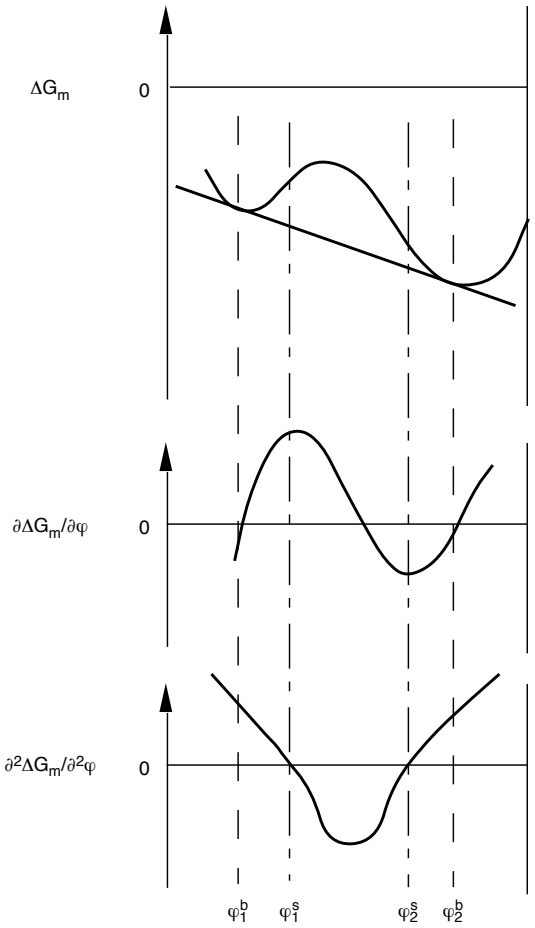

Figure 13

Gibbs free energy of a mixture and its derivatives with respect to the polymer concentration for the case of partial miscibility.

The same simple rule for polymer solubility in liquid solvent, "like dissolves like", can be applied to polymer dissolving in supercritical fluid. Thus, hydrocarbon polymers such as polyethyene are soluble in supercritical hydrocarbon such as alkenes and *n*-alkanes, while polar polymers such as polymethylmethacrylate are soluble in polar fluids such as chlorodifluoromethane. A more rigorous rule can be formulated through the Hildebrand solubility parameter, δ: a polymer should have a good solubility in a solvent if its solubility parameters are close-matched. For a supercritical fluid, the Hildebrand solubility parameter can be calculated from [117]:

$$\delta = \left((u^{ig} - u)/v\right)^{0.5} = \left((h^{ig} - RT - h + Pv)/v\right)^{0.5} \quad (23)$$

where u is the internal energy per mole, h is the enthalpy per mole, v is the molar volume and the exponent *ig* refers to ideal gas values. This description is not sufficient and many studies have been performed in order to model the polymer solubility. This will be presented hereafter.

3.1.2 Pressure effect

Generally, an increasing pressure (or density) at constant temperature makes polymer more soluble in supercritical media. All amorphous polymers, and many crystalline polymers, exhibit fluid-fluid equilibria. When the polymer-fluid solution is depressurized, it crosses the coexistence boundary and is separated into the two-phase region.

3.1.3 Temperature effect

The complete miscibility can take place upon an increase or a decrease in tempearture. This is illustrated in Figure 14 which represents systems displaying Upper Critical Solution Temperature (UCST) and Lower Critical Solution Temperature (LCST) at constant pressure. In Upper and Lower Critical Solution Temperature (U-L-CST), a two-phase solution goes to a single phase with increasing temperature, and, upon a further increase in temperature, it separates again into two phases (Table 9).

The critical concentration is an unique point for each polymer-fluid system, and at a given pressure, it is a function of the molar weight and molar weight distribution of the polymer [8].

The basic thermodynamic requirement of a negative ΔG_m would lead to the conclusion that the single phase solution is enhanced when the enthalpy of the system is negative, or when its entropy is positive enough. In UCST, an increase in solubility with an increase in temperature is associated with an endothermic heat of mixing ($\Delta H_m > 0$). When the temperature is decreased, the heat term may become larger than the entropy term and it causes phase separation. This behavior corresponds to non-polar solutions of amorphous polymers, for which the attractive forces between like molecules decrease when temperature increases and so the solubility is increased.

In LCST, the decrease in solubility with an increase in temperature is linked to an exothermic heat of mixing ($\Delta H_m < 0$). The phase separation at high enough temperature involves an unfavorable entropy effect ($\Delta S_m < 0$), which arises from the different expensivities of polymer and solvent. The polymer molecules

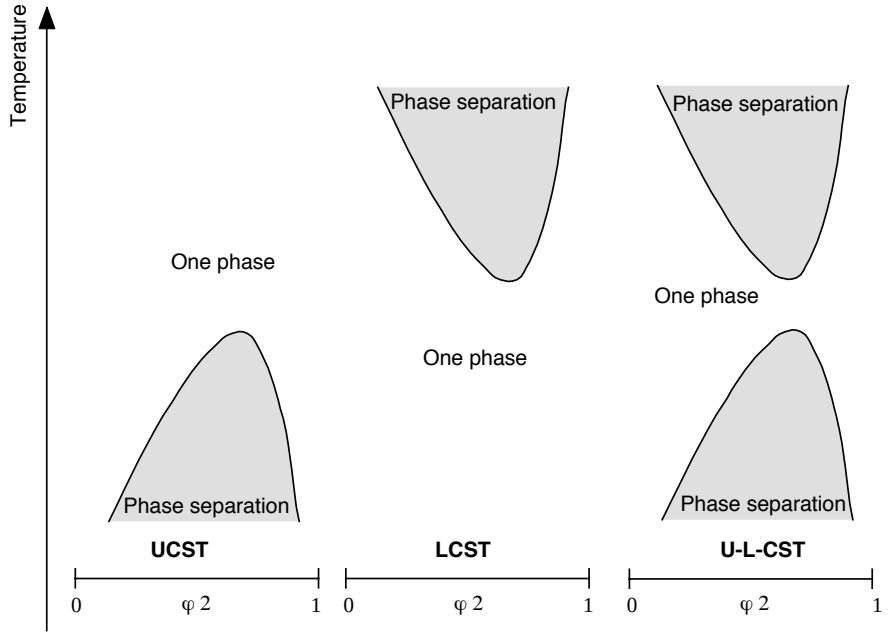

Figure 14

Binodal curves in systems displaying UCST, LCST and U-L-CST.

TABLE 9

Solubility of polymers in supercritical fluids

Polymer	M_w (kDalton)	Solvent	T (°C)	P (MPa)	$[C_p]$ (wt%)	Phase behavior	Ref.
PE	4-118	Ethylene	107-172	90-200	2-24	UCST	[164]
PE	2-420	*n*-Butane	100-200	5-30	1-10	LCST	[165]
PEP	0.8-96	Ethylene	0-200	57-172	3.8-16	ULCST	[166]
PEP	5.9	Propylene	100-150	18-30	1.8-33	LCST	[167]
PEP	69-279	*n*-Butane	135-210	60-250	5	UCST	[168]
PSt	0.4-3	Ethane	40-60	8.5-34	0.001-20	LCST	[139]
PSt	1900	Propane	50-180	25-67	0-4	UCST	[124]
PSt	22	*n*-Butane	155-201	9-13	13-26	LCST	[169]
PSt	0.5-20	R142b	120-180	6.8-40	0.03-0.2	NR	[144]
PMMA	74	$CHClF_2$	65-140	3-29	0.03-15	LCST	[170]
PDMS	135	CO_2	25-52	19.3	0.3-1	UCST	[171]
PEO	0-0.6	CO_2	40	20	0.25-1.25	NR	[148]
PEOPN	0.8-4	CO_2	45-60	12-35	0.1-7	NR	[149]

$[C_p]$ = polymer concentration; NR = not reported; PE = polyethylene; PEP = poly(ethylene-co-propylene), PSt = polystyrene; PMMA = poly(methylemethacrylate); PDMS = poly(dimethylsiloxane), PEO = poly(ethylene oxide), PEOPN = poly(ethyleneoxidenonylphenylether).

confine the solvent molecules in a more rigid matrix (solvent "condenses" around the polymer), leading to a decreasing entropy of mixing, and consequently a phase separation [118].

3.1.4 Modeling of polymer solution

The Flory-Huggins model corresponds to a rigid lattice model and the free energy of the mixture is expressed by:

$$\Delta G_m = RT\,[\ln(1-\varphi) + (1-1/n)\varphi + \chi\varphi^2] \qquad (24)$$

where φ is the volume fraction of the polymer, n represents the number of lattice sites occupied by a molecule, and χ is the Flory interaction parameter [119]. In its simplest form, the Flory-Huggins model is not capable to predict LCST and largely underestimates the critical miscibility temperature. Many modifications have been proposed in the literature but we will limit the presentation to the most used models which are the Lattice Fluid Theory of Sanchez and Lacombe [120] and [121] and a parallel approach which describes polymer solutions with a perturbation model (Statistical Associating Fluid Theory) [122] and [123].

In the Lattice Fluid Theory of Sanchez and Lacombe, the basic equation of state is:

$$\rho^2 + P + T\,[\ln(1-\rho) + (1-1/n)\rho] = 0 \qquad (25)$$

where P, T and ρ are the reduced pressure ($P/P\#$), temperature ($T/T\#$) and density ($\rho/\rho\#$), respectively, and n represents the number of lattice sites occupied by a molecule. The characteristic parameters (noted #) for the mixture are determined from the pure component values using a set of mixing rules. An adjustable binary interaction parameter δ_{ij} is introduced for each binary pair.

To determine the phase diagrams or the binodal curves, the method involves the determination of densities which verify the equilibrium conditions (chemical potentials of the components in each phase become equal). The spinodal curves are determined from the condition $\partial m/\partial j = 0$. This model has been used to describe the behavior of polyethylene in n-pentane and in n-pentane-carbon dioxide solutions at high pressures [124].

Predictions are shown to be in good agreement with the experimental demixing data and correctly describe the LCST and UCST behaviors. However, if the characteristic temperature of the polymer is not adjusted, the model does not perform well and greatly overestimates the demixing pressures in both pure and binary solvents [8].

In the Statistical Associating Fluid Theory (SAFT), the general expression for the residual Helmholtz energy is a combinaison of a reference part, made up of contributions from hard sphere (*hs*), chain, and association (*assoc*) terms, and a dispersion (*disp*) part:

$$a^{res} = a^{ref} + a^{disp} \qquad (26)$$

$$a^{ref} = a^{hs} + a^{chain} + a^{assoc} \qquad (27)$$

Each of the above contributions can be expressed as a function of known quantities and of three molecular parameters: the number of segments per molecule, the segment volume per mole of segments and the segment energy. In addition, one adjustable binary interaction parameter can be necessary, k_{ij}, and is adjusted to fit the experimental data.

The prediction of the phase boundaries of the polyethylene-*n*-pentane system is remarkable for a k_{ij} set equal to zero [122]. For polystyrene-propane system, it was found to be able to accurately calculate the composition of both phases with a k_{ij} depending only on T and P [124]. The SAFT model, while more cumbersome to implement than the Lattice Fluid Theory, is especially well suited for polymers with varying backbone architecture, such as branched polymers or copolymers [125].

3.1.5 Polymer-fluid system

Table 9 summarizes the polymer-fluid solutions whose phase behavior has been experimentally characterized. The solubility of polymers in a supercritical solvent is limited and in some case, the pressure required for dissolution are extremely high. A good liquid solvent (at ambient conditions) may be added to the supercritical fluid as a cosolvent to enhance the solubility.

Dissolution of polymers in supercritical fluids is performed in polymerization as previously discussed, in separation processes (see chap. 3.2) and in the rapid expansion of supercritical solutions (RESS) [15] and [16]. The expansion process time can be less than 10^{-5} second and then allows to produce solid particles with a narrow size distribution and different properties: modification of morphology, crystallization and increase in melting point [126].

This technique is used, in particular, to produce bioerodible polymeric microspheres loaded with a therapeutic drug, a composite suitable for controlled delivery applications [127] and [128].

Supercritical carbon dioxide dissolves a quite small number of polymers but the carbon dioxide is readily sorbed into a wide variety of polymers at elevated pressures [129]. For a given polymer, the glass transition temperature (T_g) is all the more decreased as the amount of carbon dioxide adsorbed increases as shown in Table 10.

TABLE 10

Decrease of glass transtion temperature (*Tg*) of some polymers by high pressure in CO_2

Polymer	$T_{g,o}$ (°C)	Pressure (MPa)	$T_{g,P}$ (°C)	ΔT_g (°C)	Ref.
Polystyrene	100	2.03	78	22	[172]
	100	6.08	35	65	[173]
Poly(methylmethacrylate)	105	3.75	75	30	[174]
	105	6.08	45	60	[174]
Poly(vinyl chloride)	75	2.03	57	18	[172]
Polycarbonate	148	2.03	97	51	[172]
Poly(vinylidene fluoride)	105	2.03	60	45	[172]
Polyimide	227	6.08	0	227	[175]

$T_{g,o} = T_g$ at ambient pressure

The plasticization effect of carbon dioxide on polymers has been used to facilite impurity extraction, to form microcellular foams [130] and [131] and as drying agent. Polymer microspheres and fibers are produced by precipitation with a compressed fluid antisolvent (PCA) [132]. Here, a polymer in a liquid solvent is sprayed across a small capillary into a vessel containing a compressed fluid, such as carbon dioxide. Carbon dioxide is miscible with the solvent, such as toluene, but is an antisolvent for the polymer. For example, microcellular poly(methacrylate) have been generated by supercritical carbon dioxide [133].

3.2 Separation process

In general, synthetic polymers have broad molar mass distribution due to unreacted monomers or oligomers in medium which can induce dramatical consequences on material properties required for particular applications.

Anionic living polymerizations give materials with a narrow polydispersity, but they require strict purity conditions and high costs. Then, from an industrial point of view, free radical polymerizations (which lead to broad molar mass distribution) followed by a fractionation or an extraction (monomers, residual solvent, etc.) step are preferred. That is why supercritical purifications have been studied and sometimes applied as industrial processes.

3.2.1 Molar weight fractionation

Many studies have been recently devoted to processes using SCF [134] and [135]. An important application of SCF is the fractionation of a broadly distributed polymer into narrow fractions [4, 136, 137, 138, 139, 140, 141, 142, 143, 144, 145, 146]. In the fractionation of a given polymer, the main parameter is the separation factor which is the ratio between the equilibrium concentrations of an *i*-mer (a polymer with an *i* degree of polymerisation) in the coexisting two phases [119]. The mass-based partition coefficient can be described by the following equation [147]:

$$\text{Log}(w'_i/w_i) = \text{Log}\, K_i = -\sigma M_i + \beta \qquad (28)$$

K_i factor, which represents the ratio between the mass fraction of the *i*-mer, with a molar mass of M_i, in the solvent rich phase (w'_i) and its mass fraction in the polymer rich phase (w_i), is a function of both temperature and pressure at which the fractionation is carried out. The *i*-mer solubility is controlled by the medium density and increases with this latter one. At constant pressure and temperature, the variation of K_i factor only depends on the molar mass of the *i*-mer (M_i) in an exponential way. The selectivity of the separation is related to σ and decreases with pressure at constant temperature [139, 144, 148]. The constant β is related to the ratio between the volumes of the coexisting phases [119].

Fractionation of PEO has been performed in supercritical carbon dioxide [148]. The highest solubilized M_i is up to 850 g/mol and Log K_i vs M_i is linear if M_i exceeds 400 g/mol. Below this critical value, the effects due the end-groups are responsible for the unexpected behavior of the mass-based partition coefficient. As shown in Figure 15, same results have been obtained on poly(ethyleneoxidenonylphenylether)-CO_2 system with

a higher molar mass solubilized of 3500 g/mol for a pressure of 30 MPa [149].

The linear variation of Log K_i vs M_i is also validated for systems polystyrene-low-hydrocarbon [139] and polystyrene-1 chloro 1-1 difluoroethane [150].

The real interest in supercritical fluid fractionation is due to the possible continuous adjustement of ratio solubility/selectivity from a quite total solubility of all chains but without any selectivity (in liquid phase) to a solubility of monomers only at very low concentration (in gas phase).

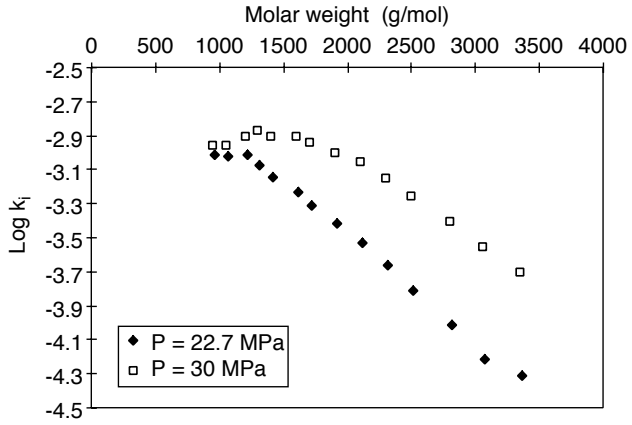

Figure 15

Coefficient partition evolution for poly(ethyleneoxide nonyl phenyl ether)-CO_2 system as a function of the molar weight at 45°C [149].

Moreover, the mass-transfer is enhanced, since natural convection effects are inversely proportional to the square of the kinematic viscosity ($\nu = \eta/\rho$; η and ρ are viscosity and density of fluid respectively) which is very low in the supercritical region [151]. However, the fractionation of an *i*-mer becomes more difficult when this *i*-mer concentration in the polymer rich phase decreases as shown by equation (28).

This phenomena is classically observed in liquid extraction. Equation (28) shows that K_i is then quite constant, which means that the transfer in the fluid phase (represented by w'_i) decreases with w_i. As a result, the last residual amounts of impurities are difficult to extract. From a general point of view, the best process for material purification consists in extracting by supercritical fluid most of the interesting product so as to obtain it as pure as possible, the species remaining in the stationary phase being mainly impurities.

The solubility of poly(ethylene-co-3.9% mol acrylic acid) ($EAA_{3.9}$) in butane, butene and dimethyl ether has been studied [152] and [153]. Two approachs are considered: the first one consists in begining the experiment with the best solvent, which is dimethyl ether. The second method consists in begining with a poorest solvent which is butane, continuing with butene and finishing with dimethyl ether. In the first case, the fractionation is obtained as a function of the molecular weight (five fractions with narrow polymolecularity are recovered). Indeed, the high hydrogen boundings between acid groups and the solvent do not permit any separation based on chemical composition. In the second case, the fractionation is followed with respect to the chemical composition: butane allows to recover 20% of copolymer chains containing 2.7% mol acrylic acid (the non-polar butane rather interact with oligomers rich in non-polar ethylene units) wheras dimethyl ether gives fractions containing about 3.5% mol acrylic acid units.

The nature of solvent influences the fractionation of polyethylene: supercritical CO_2 is a poor solvent but is very selective, supercritical propane is a good solvent but is no selective. A mixture made with 80% in volume of CO_2 and 20% in volume of propane [154] allows to reach a good compromise between solubility and selectivity.

A new fractionation technique, named critical isobaric temperature rising elution fractionation (CITREF) has been developed [142] and [155]. This separation method is based on the selective recrystallization. It leads to a fractionation according to backbone structure rather than molecular weight. A semi-crystalline linear, as low density polyethylene, can be fractionated according to both molecular weight and backbone structure by a double fractionation: an isothermal increasing pressure profile at 130°C followed by a CITREF.

3.2.2 Architecture fractionation

The fractionation of a binary mixture (noted M_1) made of three-arm stars of polyethyleneoxide (PEO) (*Mn* = 2 800 g/mol) and of linear chains of PEO (*Mn* = 900 g/mol) was thus attempted [4]. In this case, the contaminating chain was chosen so as to exhibit the same molar mass as that of the star branches. In the

binary mixture (M_1), the content in linear materials was purposely raised to 50% in weight so as to investigate the selectivity of this fractionation technique. The separation of the linear chain (*Mn* = 900 g/mol) from the star structure (*Mn* = 2 800 g/mol) occurs upon applying a pressure of 6 MPa shown that linear chains of 900 g/mol are selectively extracted. The separation of two different architectures can be used as a preparative method. Indeed, the purification of 1 g of star/linear mixture with *Mn* = 2 800 g/mol was completed in 80 min with a flow rate of fluid of 10 ml/min. The amount of purified PEO star recovered in the mass exchanger is above 90%. These results are remarkable when compared to other techniques of fractionation (dialyse or SEC) which either take much more time or only afford very small amounts of fractionated polymers [4].

Another case involving star molecules and linear chains was also investigated. A binary mixture containing PEO star and linear of about the same molar mass was then investigated [4]. The separation of linear from star polymers has been performed with an efficiency higher than 90% in weigh. The partition process cannot be interpreted as being due to steric exclusion but rather to a solubility process that depends on the fluid density and the hydrodynamic volume of the polymer at a given temperature. The *i*-mer solubility increases with fluid density at constant temperature as previously discussed. When applied to polymers in supercritical fluid, models such as the statistical associating fluid theory (SAFT) [122] or the Sanchez-Lacombe theory [120] indeed predict such a behavior.

These models show that the demixing pressures on polymers in supercritical fluids increase with the molar mass of the sample. The Sanchez-Lacombe model defines the intermolecular and intramolecular interactions and the close-packed volume of an *i*-mer. The intramolecular interactions for the star structure are expected to be higher than for the linear structure of same molar mass giving rise to a low hydrodynamic volume on the star structure than on the linear chain. As evidenced by steric exclusion chromatography, star structures exhibiting the same molar mass as that of a linear equivalent is eluted at higher elution times. Because of its lower hydrodynamic volume, the star structure exhibits a lower apparent mass. Therefore, this star macromolecule will be solubilized at a lower pressure than would be its homologous linear structure. The point that really matters for separation by supercritical fluids is the hydrodynamic volume of the different species to fractionate. In other words, two polymers with the same chemical nature and molar masses but different topologies can be separated off, provided their respective molecular dimensions strongly differ. The driving force for an effective separation by supercritical fluids depends on the temperature and density of the solvent, and on the hydrodynamic volume of the polymer rather than its molar mass.

Several teams have performed to separate polymers with different structures. This fractionation type is based on the hydrodynamic volume differences between macromolecular chains. Cyclic oligomers present during the α-ω carboxylpropylpoly(dimethyl) siloxane formation have been extracted with supercritical CO_2 [136] and [137].

The supercritical fractionation depends also on the physic state of the polymer: high and low density polyethylenes have been fractionated in supercritical propane, on the basis of cristallinity differences. Then the recovered fractions have a more homogeneous structure than the parent polymer [142] and [155].

3.3 Impregnation process

Swelling of the polymer by supercritical fluid effectively increases the diffusion coefficient of heavy dopant by several orders of magnitude. When the system is depressurized, the dissolved fluid readily diffuses from the polymer while the heavy dopant, which is trapped in the matrix, slowly diffuses out of the solid at a rate of several orders of magnitude slower than the rate it was put into the polymer. This technique can be used to form novel controlled-release devices. Indeed, very large molecules can be impregnated into a swollen polymer matrix at operating temperature low enough to avoid thermal degradation of materials.

Polymers can be impregnated by substrates as pharmaceuticals, fragrances or other additives which are solubilized in the supercritical fluid, or impregnated only by the supercritical fluid. These processes allow to modify polymer properties as plasticization effects (decrease of glass transition temperature). Supercritical CO_2 is used, in these experiments, because of its non-toxic charasteristics and its high capacity to be solubilized in many polymers [156]. This peculiar behaviour is explained and detailed in many publications [157, 158, 159]. As exemple, vinylic

monomers are impregnated in wood polymers by the supercritical CO_2 and in a second time polymerized to improve mechanical properties [160].

3.4 Recycling process

The aim of the chemical recycling of polymer by supercritical fluids is to recover the monomers from the polymer materials at the "end of their life" [11, 12, 161, 162, 163]. Supercritical fluids are able to modify the chemistry equilibria by action of pressure and temperature as previously discussed. The solubility and selectivity parameters can be adjusted so that only the monomers are solubilized and coeluted with the fluid. As a consequence the chemical equilibrium between polymers-oligomers-monomers is shifted to monomer formation. Moreover, due to the ability of the fluid to plastify the polymer matrix, the polymer attack is favored. As an exemple, polyamide recycling is performed by ammonolysis in ammonia [161]. The best recycling efficiency is obtained for a mixture of polyamide 6 and 6,6 in protonic medium ($(NH_4)_2HPO_4$) at 330°C and 13 MPa. This provides an overall yield to monomeric products of 81%.

CONCLUSION

The industrial and scientific interest in supercritical fluids are linked with the capability of some supercritical fluids for replacing toxic industrial solvents and the possibility to make new processes at mild conditions. The supercritical fluid processes development requires the knowledge of thermodynamic data such as Equations of State, of thermophysic data such as viscosity and diffusivity and also of chemical data such as enthalpy of reaction.

However, a separation process carried out by traditional methods, such as liquid extraction or adsorption, is generally less expensive than a supercritical fluid process. Indeed, the solubility of a solute in a supercritical fluid can be decreased of many orders of magnitude in relation to the fluid density and the nature of solvent which is generally different from the liquid one. Moreover, the cost due to the compression and the containment of the fluid may limit the economic feasibility of the supercritical fluid extraction. So high investment cost can be performed for large-scale productions or for small-scale productions if the product is very expensive. Common examples include large-scale operations such as the production of low density polyethylene, mid-scale operations such as the tea and hops extractions, and small-scale batchwise operations such as spices and fragrances extractions.

The major application areas for the further development of supercritical fluid will be located in two main domains: the first one deals with materials processing such as polymer processing, ceramics, surface coating, particle formation, impregnation and dying; the second one deals with environmental applications such as wastes treatment, materials recycling and soil remediation. These application areas will be developped only if the characteristics and specifications of supercritical processes cannot be obtained by other means at ambient pressure.

ACKNOWLEDGEMENTS

The authors express their gratitude to C. Brugne for her contribution.

REFERENCES

1 Hutchenson K.W. and Foster N.R. (1995) Innovations in supercritical fluids. *ACS Symposium*, Serie 608, Washington.

2 Akgerman A. and Madras G. (1994) Supercritical fluids-Fundamentals for application. *Nato ASI Ser*. E 273, Kluwer, Dordrecht, 669-695.

3 McHugh M.A. and Krukonis V.J. (1998) S*upercritical Fluid Extraction: Principles and Practice*. Butterworths, Stoneham, MA.

4 Cansell F., Botella Ph., Garrabos Y., Six J.L., Gnanou Y. and Tufeu R. (1997) *Polymers J*., 29, 910-916.

5 Beckman E.J. (1996) Nature 271, 613-614.

6 Page S.H., Morrison J.F. and Lee M.L. (1994) Supercritical fluids-Fundamentals for application. *Nato ASI Ser*. E 273, Kluwer, Dordrecht, 641-652.

7 Schneider G.M. (1983) *Fluid Phase Equilib*. 10, 141-157.

8 Kiran E. (1994) Supercritical fluids-Fundamentals for application. *Nato ASI Ser*. E 273, Kluwer, Dordrecht, 541-588.

9 Savage P.E., Gopalan S., Mizian T.I., Martino C.J. and Brock E.E. (1995) *AIChE J*., 41, 1723-1778.

10 Beslin P., Cansell F., Garrabos Y, Demazeau G., Berdeu B. and Sentagnes D. (1997) *Déchets*, 5, 17-21.

11 Chen D.T., Craig A.P., Reichert E., Hoven J. and J. Hazar. (1995) *Mat*. 44, 53-60.

12 Lentz H. and Mormann W. (1992) Makromol. Chem. *Macromol. Symp.*, 57, 305-310.

13 Johnston K.P., Harrison K.L., Clarke M.J., Howdle S.M., Heitz M.P., Bright F.V., Carlier C. and Randolph T.W. (1996) *Nature*. 271, 624-626.

14 Petitet J.P. (1995) Fluides supercritiques et matériaux. *AIPFS* Publishing Nancy, 251-300.

15 Debenedetti P.G. (1994) Supercritical fluids-Fundamentals for application. *Nato ASI Ser.* E 273, Kluwer, Dordrecht, 719-729.

16 Ksibi H. and Subra P. (1996) *Advanced Powder Technol.* 7, 21-28.

17 Chhor K., Bocquet J.F. and Pommier C. (1995) *Mat. Chem. Phys.* 40, 63-68.

18 Beslin P., Jestin P., Desmarest Ph., Tufeu R. and Cansell F. (1994) Third inter. symp. on supercritical fluids. *AIPFS* Publishing Nancy, 3, 321-326.

19 Laudise R.A. and Johnson D.W. (1986) *J. Non Crystalline Solids*, 79, 155-164.

20 Rangarajan B. and Lira C.T. (1991) *J. Supercritical Fluids*, 4, 1-6.

21 Levelt Sengers J.M.H. (1994) Supercritical fluids-Fundamentals for application. *Nato ASI Ser.* E 273, Kluwer, Dordrecht, 3-38.

22 Schmidt E. (1982) *Properties of Water and Steam in SI-Units*, Ed Grigull U., Springer-Verlag, New York.

23 Lee L. and Cochran H.D. (1994) Supercritical fluids-Fundamentals for application. *Nato ASI Ser.* E 273, Kluwer, Dordrecht, 365-383.

24 Cabaço M.I., Danten Y., Besnard M., Bellissent-Funel M.C., Guissani Y. and Guillot B. (1997) Molecular Physics, 90, 817-828.

25 Cabaço M.I., Danten Y., Besnard M., Guissani Y. and Guillot B. (1997) *Molecular Physics*, 90, 829-840.

26 Eckert C.A., Knutson B.L. and Debenedetti P.G. (1996) Nature. 383, 313-318.

27 Sengers J.V. and Levelt Sengers J.M.H. (1986) *Annu. Rev. Phys. Chem.*, 37, 189-222.

28 Vargaftik N.B. (1975) Table on the *Thermophysical Properties of Liquids and Gases*, Hemisphere Publishing Corporation, London.

29 Svensson P. (1995) *Chemical Technology*, 2, 16-19.

30 Debenedetti P.G. and Reid R.C. (1986) *AIChE J.*, 32, 2034-2046.

31 Petsche I.B. and Debenedetti P.G. (1991) *J. Phys. Chem.*, 95, 386-399.

32 Eckert C.A., Ziger D.H., Johnston K.P. and Kim S. (1986) *J. Phys. Chem.*, 90, 2738-2746.

33 Czubryt J.J., Myers M.N. and Giddings J.C. (1970) *J. Phys. Chem.*, 74, 4260-4266.

34 Franck E.U. (1956) *Z. Phys. Chem.*, 6, 345-355.

35 Rowlinson J.S. and Richardson M.J. (1959) *Adv. Chem. Phys.*, 2, 85-118.

36 Reid R.C., Prausnitz J.M. and Sherwood T.K. (1977) *The Properties of Gases and Liquids*, Mc Graw-Hill, New York.

37 Chrastil J. (1982) *J. Phys. Chem.*, 86, 3016-3021.

38 Pouillot F., Dillow-Wilson A.K. and Eckert C.A. (1995) Fluides supercritiques et matériaux. *AIPFS* Publishing Nancy, 60-109.

39 Marteau Ph., Tobaly P., Ruffier-Meray V. and Barreau A. (1996) *Fluid Phase Equil.*, 119, 213-230.

40 Chialvo A.A. and Cummings P.T. (1994) *AIChE J.*, 40, 1558-1573.

41 Brennecke J.F., Debenedetti P.G., Eckert C.A. and Johnston K.P. (1990) *AIChE J.*, 36, 1927-1934.

42 Carlier C. and Randolph T.W. (1993) *AIChE J.*, 39, 876-884.

43 O'Brien J.A., Randolph T.W., Carlier C. and Ganapathy S. (1993) *AIChE J.*, 39, 1061-1071.

44 Debenedetti P.G. and Chialvo A.A. (1992) *J. Chem. Phys.*, 97, 504-507.

45 Eckert C.A. and Knuston B.L. (1993) *Fluid Phase Equi.*, 83, 93-100.

46 Tom J.W. and Debenedetti P.G. (1993) *Ind. Eng. Chem. Res.*, 32, 2118-2128.

47 Petsche I.B. and Debenedetti P.G. (1989) *J. Chem. Phys.*, 91, 7075-7084.

48 Gurdial S. G., Macnaugthon S.J., Tomasko D.L. and Foster N.R. (1993) *Ind. Eng. Chem. Res.*, 32, 1488-1497.

49 Chivalo A.A. (1993) *J. Phys. Chem.*, 97, 2740-2744.

50 Ekart M.P., Bennet K.L., Ekart S.M., Guardial S. G., Liotta C.L. and Eckert C.A. (1992) *AIChE J.*, 39, 235-248.

51 Wheeler J.C. (1972) *Ber. Bunsenges. Phys. Chem.*, 76, 308-318.

52 Kurnik R.T. and Reid R.C. (1982) *Fluid Phase Equil.*, 8, 93-105.

53 Dong D.C. and Winnick M.A. (1984) *Photo. Chem. Photobio.*, 35, 17-21.

54 Brennecke J.F., Tomasko D.L., Peshkin J. and Eckert C.A. (1990) *Ind. Eng. Chem. Res.*, 29, 1682-1690.

55 Kim S. and Johnston K.P. (1987) *AIChE J.*, 33, 1603-1611.

56 Yonker C.R. and Smith R.D. (1988) *J. Phys. Chem.*, 92, 2374-2378.

57 Phillips D.J. and Brennecke J.F. (1993) *Ind. Eng. Chem. Res.*, 32, 943-941.

58 Fulton J.L., Yee G.G. and Smith R.D. (1991) *J. Am. Chem. Soc.*, 113, 8327-8334.

59 Gupta R.M., Combes J.R. and Johnston K.P. (1993) *J. Phys. Chem.*, 97, 707-715.

60 Hicks C.P. and Young C.L. (1975) *Chem. Rev.*, 75, 119-174.

61 Tromp R.H., Postorino P., Neilson G.W., Ricci M.A. and Soper A.K. (1994) *J. Chem. Phys.*, 101, 6210-6214.

62 Ohtaki H., Radnai T. and Yamaguchi T. (1997) *Chem. Soci. Rev.*, 41-51.

63 Connolly J.F. (1996) *J. Chem. Eng. Data*, 11, 13-16.

64 Tester J.W., Holgate H.R., Armellini F.J., Webley P.A., Killilea W.R., Hong G.T. and Barner H.E. (1993) Emerging technologies in hazardous waste management III. *ACS Symp. Ser.* 518, 35-76.

65 Modell M. (1982) *US Patent*. 4, 338,199.

66 Gearhart J.A. and Garwin L. (1976) *Hydrocarbon Proc.*, 5, 125-129.

67 Atkins P.W. (1990) *Physical Chemistry*, Oxford University Press, Oxford, 850-862.

68 Eckert C.A., Hsieh C.K. and McCabe J.R. (1974) *AIChE J.*, 20, 20-36.

69 Van Eldik R., Asano T. and Le Noble W.J. (1989) *Chem. Rev.*, 89, 549-688.

70 Simmons G.M. and Masson D.M. (1972) *Chem. Eng. Sci.*, 27, 89-108.

71 Kistiatowsky G.B. (1928) *J. Am. Chem. Soc.*, 50, 2315-2336.

72 Kondo Y. (1968) *Bull. Chem. Soc. Japan*, 41, 987-992.

73 Dooley K.M., Brodt S.R. and Knopf F.C. (1987) *Ind. Eng. Chem. Res.*, 26, 1267-1267.

74 Johnston K.P. and Haynes C. (1987) *AIChE J.*, 33, 2017-2026.

75 Randolph T.W. and Carlier C. (1992) *J. Phys. Chem.*, 96, 5146-5151.

76 Flarsheim W.M., Bard A.J. and Johnston K.P. (1989) *J. Phys. Chem.*, 93, 4234-4242.

77 Wu B.C., Klein M.T. and Sandler S. (1991) *Ind. Eng. Chem. Res.*, 30, 822-829.

78 Subramaniam B. and McHugh M.A. (1986) *Ind. Eng. Chem. Process Des. Dev.*, 25, 1-12.

79 Clifford A.A. (1994) Supercritical fluids-Fundamentals for application. *Nato ASI Ser.* E 273, Kluwer, Dordrecht, 449-480.

80 Thies H. (1978) *Chimia*, 32, 79-89.

81 Scholsky K.M. (1993) *J. Supercriti. Fluids*, 6, 103-127.

82 Krase N.M. and Lauwrence A.E. (1946) *US Patent*, 2, 396, 791.

83 Saraf V.P. and Kiran E. (1990) *Polymer Preprints*, 31, 687-688.

84 De Simone J.M., Maury E.E., Menceloglv Y.Z., Mc Clain J.B., Romack T.J. and Combes J.R. (1994) *Science*, 265, 356-359.

85 De Simone J.M., Guan Z. and Elsbernd C.S. (1992) *Science*, 257, 945-947.

86 Odell P.G., Hamer G.K. and Georges M.K. (1996) *E. Patent*, 0, 735, 051 A1.

87 Adamsky F.A. and Beckman E.J. (1994) *Macromolecules*, 27, 312-314.

88 Russel A.J., Beckman E.J., Abderrahmare D. and Chauhary A.K. (1995) *US Patent*, 5, 478, 910.

89 Mistele C.D., Thorp H.H. and De Simone J.M. (1995) *Polymer Preprints*, 36, 507-508.

90 Shaw R.W., Brill T.B., Clifford A.A., Eckert C.A. and Franck E.U. (1991) *Special Report C&EN*, 69, 26-39.

91 Modell M. (1985) *US Patent*, 4, 453, 190.

92 Kläy H.R. (1989) *Info. Chimie*, 308, 195-197.

93 Helling R.K. and Tester J.W. (1988) *Environ. Sci. Technol.*, 22, 1319-1324.

94 Beslin P., Cansell F., Garrabos Y., Demazeau G., Berdeu B. and Sentagnes D. (1997) Supercritical fluids and environment. *AIPFS* Publishing Nancy, 11-16.

95 Joussot-Dubien Ch. (1996) *PhD Thesis.* University of Bordeaux I, France.

96 Yang H.H. and Eckert C.A. (1988) *Ind. Eng. Chem. Res.*, 27, 2005-2014.

97 Lee D., Gloyna E.F. and Lixiong L. (1990) *J. Supercrit. Fluids*, 3, 249-255.

98 Thornton T.D. and Savage P.E (1990) *J. Supercrit. Fluids*, 3, 240-248.

99 Antal M.J. (1995) *Proc. Int. Conf. Prop. Water Steam 12th*, Publisher Begell House, New York, 24-32.

100 Holgate H.R, Tester J.W. and Meyer J.C. (1995) *AIChE*, 41, 637-648.

101 Tester J.W., Webley P.A. and Holgate H.R (1993) *Ind. Eng. Chem. Res.*, 32, 236-239.

102 Krajnc M. and Levec J. (1994) *Applied Catalysis B: Environmental*, 3, L101-L107.

103 Li R., Thornton T.D. and Savage P.E (1992) *Environ. Sci. Technol.*, 26, 2388-2395.

104 Gopalan S. and Savage P.E. (1995) *AIChE J.*, 41, 1864-1873.

105 Krajnc M. and Levec J. (1997) Proceedings of 1st European congress on chemical engineering. *AIDIC* Publishing Milano, 1, 425-428.

106 *Eco Waste Technologies, Information package,* Austin Texas 78758.

107 Modell M., Larson J., Sobczynski S.F. and Tappi J. (1992) 195-202.

108 Beslin P., Cansell F., Berdeu B., Garrabos Y. and Demazeau G., Sentagnes (1997) Proceedings D., 1st European congress on chemical engineering. *AIDIC* Publishing Milano, 1, 651-654.

109 Goldacker H., Abeln J., Kluth M., Kruse A., Schmieder H. and Wiegand G. (1996) High pressure chemical engineering. *Process Technology Proceeding*, Elsevier, Amsterdam, 12, 61-66.

110 Lixiong L., Gloyna E.F. and Sawicki J.E. (1993) *Water Environment Research*, 65, 250-257.

111 Luck F., Bonnin C., Niel G. and Naud G. (1995) *First International Workshop on Supercritical Water Oxidation*, Session X, Jacksonville, USA, 25-31.

112 Shanableh A. and Gloyna E.F. (1991) *Wat. Sci. Tech.*, 23, 389-398.

113 Timberlake S.H., Hong G.T., Simson M. and Modell M. (1982) *SAE Tech. Pap. Ser.*, n° 820872.

114 Johnston J.B., Hannah R.E., Cunningham V.L., Daggy B.P., Sturm F.J. and Kelly R.M. (1988) *Biotechnology*, 6, 1423-1427.

115 Harradine D.M., Buelow S.J., Dell'orco P.C, Dyer R.B., Foy B.R., Robinson J.M., Sanchez J.A, Spontarelli T. and Wander J.D. (1993) *Hazardous Waste & Hazardous Materials*, 10, 233-246.

116 Hazlebeck D.A., Downey K.W., Jensen D.D. and Spritzer M.H. (1993) *Report General Atomics*, March.

117 Johnston K.P. (1989) Supercritical fluid science and technology. *ACS Symp.*, 406, 1-12.

118 Somcynski T. and Simha R. (1971) *J. Appl. Phys.*, 42, 4545-4548.

119 Flory P.J. (1953) *Principles of Polymer Chemistry*, Cornell University Press: Ithaca, New York, Chapters 12, 13.

120 Sanchez I. and Lacombe R.H. (1976) *J. Phys. Chem.*, 80, 2352-2362.

121 Sanchez I. and Lacombe R.H. (1978) *Macromolecules*, 11, 1145-1156.

122 Huang S.H. and Radosz M. (1990) *Ind. Eng. Chem.*, 29, 2284-2294.

123 Huang S.H. and Radosz M. (1991) *Ind. Eng. Chem.*, 30, 1994-2005.

124 Pradhan D., Chen C.K. and Radosz M. (1994) *Ind. Eng. Chem. Res.*, 33, 1984-1988.

125 Shine A.D. (1996) *Physical Properties of Polymers Handbook*, 249-256.

126 Lele A.K. and Shine A.D. (1990) *Polymer Preprints*, 31, 677-678.

127 Debenedetti P.G., Tom J.W., Kwauk X. and Yeo S.D. (1993) *Fluid Phase Equilibria*, 82, 2304-2310.

128 Tom J.W., Lim G.B., Debenedetti P.G. and Prud'Homme R.K. (1993) *Supercritical Engineering Science Fundamentals and Applications*, 238-257.

129 Shieh Y.T., Su J.H., Manivannan G., Lee P.H.C., Sawan S.P. and Spall W.D. (1996) *J. Appl. Polym. Sci.*, 59, 695-705 and 707-717.

130 Goel S.K. and Beckman E.J. (1994) *Polym. Eng. Sci.*, 34, 1137-1147.

131 Goel S.K. and Beckman E.J. (1994) *Polym. Eng. Sci.*, 34, 1148-1156.

132 Dixon D.J. and Johnston K.P. (1993) *J. Appl. Polym. Sci.*, 50, 1929-1942.

133 Goel S.K. and Beckman E.J. (1993) *Cellular Polymers*, 12, 251-274.

134 Cansell F. and Petitet J.P. (1995) Fluides supercritiques et matériaux. *AIPFS* Pub. Nancy.

135 Garrabos Y., Le Neindre B., Subra P., Cansell F. and Pommier C. (1992) *Ann. Chim. Fr.*, 17, 55-90.

136 Yilgor I., Mc Grath J.E., and Krukonis V.J. (1984) *Polym. Bull.*, 12, 491-497.

137 Yilgor I., McGrath J.E., Krukonis V.J. (1984) *Polym. Bull.*, 12, 499-506.

138 Krukonis V.J. (1985) *Polym. News*, 11, 7-16.

139 Kumar S.K., Chhabria S.P., Reid R.C. and Suter U.W. (1987) *Macromolecules*, 20, 2550-2557.

140 Scholsky K.M., O'Connor V.M. and Weiss C.S. (1987) *J. Appl. Polym. Sci.*, 33, 2925-2934.

141 Schmitz F.P. and Klesper E.J. (1990) *J. Supercrit. Fluids*, 3, 29-48.

142 Watkins J.J., Krukonis V.J., Condo P.D., Pradham D. and Ehrlich P.J. (1991) *J. Supercrit. Fluids*, 4, 24-31.

143 Kiran E and Zhuang (1992) *Polymer J.*, 33, 5259-5263.

144 Desmarest Ph., Hamedi M., Tufeu R. and Cansell F. (1994) *Third Inter. Symp. on Supercritical Fluids*, 3, 287-290.

145 Radosz M., Banaszak M., Chen C.K. and Gregg C.J. (1994) Third inter. symp. on supercritical fluids. *AIPFS* Publishing Nancy, 3, 279-280.

146 Cansell F., Botella Ph., GarrabosY., Six J.L., Gnanou Y. and Tufeu R. (1997) Supercritical fluids and environment. *AIPFS* Publishing Nancy, 75-79.

147 Koningsveld R., Stockmayer W.H., Kennedy J.W. and Kleintjens L.A. (1974) *Macromolecules*, 7, 73-79.

148 Daneshwar M. and Gulari E. (1992) *J. Supercrit. Fluids*, 5, 143-150.

149 Dimitrov K., Boyadzhiev L., Subra P., Tufeu R. and Cansell F. (1997) Supercritical fluids and environment. *AIPFS* Publishing Nancy, 169-172.

150 Hamedi M., Desmarest Ph., Tufeu R. and Cansell F. (1997) *Polymer*, 39, 347-353.

151 Debenedetti P.G. and Reid R.C. (1986) *AIChE J.*, 32, 2034-2046.

152 McHugh MA., Krukonis V and Pratt J.A. (1994) *Trends Polymer Science*, 29, 301-307.

153 Meilchen M.A., Hasch B.M. and McHugh M.A. (1991) Second inter. symp. on supercritical fluids. *AIPFS* Publishing Nancy, 41-44.

154 Via S.C., Brave C.L. and Taylor L.T. (1994) *Annl. Chem.*, 66, 603-609.

155 Smith S.D., Satkowski M., Ehrlich P., M.Watkins J.J. and Krukonis V. (1991) *Polymer Preprints*, 32, 291-292.

156 Berens A.R., Huvard G.S. and Korsmeyer R.W. (1988) *AIChE Annual Meeting*, 2.

157 Berens A.R. and Huvard G.S. (1989) *ACS Symp. Ser.* 406, 207-223.

158 Liau I.S. and McHugh M.A. (1985) *Supercritical Fluid Technology*, Elsevier, Amsterdam, 415-434.

159 Shim J.J. and Johnston K.P. (1990) *Polymer Preprints*, 31, 681-682.

160 Kiran E. (1995) *ACS Symposium Series*, 608, 380-401.

161 McKinney R.J. (1994) *US Patent E.I. Du Pont de Nemours and Compagny: Apr. 12*, 5, 302, 756, *Mar. 7* (1995), 5, 395, 974.

162 Blackmon K.P., Fox D.W. and Shafer S.J. (1990) *US Patent General Electric Compagny: Nov. 27*, 4, 973, 746.

163 Lee S., Gencer M.A., Fullerton K.L. and Azzam F.O. (1995) *US Patent University of Akron: Jan. 31*, 5, 386, 055.

164 De Loos T.W., Poot W. and Diepen G.A.M. (1983) *Macromolecules*, 16, 111-117.

165 Xiong Y. and Kiran E. (1993) *J. Appl. Polym. Sci.*, 47, 895-909.

166 Gregg C.J., Chen S.J., Stein F.P. and Radosz M. (1993) *Fluid Phase Equilibria*, 83, 374-382.

167 Gregg C.J., Stein F.P., Morgan C.K. and Radosz M. (1994) *J. Chem. Eng. Data*, 39, 219-224.

168 Lee S.H., LoStracco M.A. and McHugh M.A. (1994) *Macromolecules*, 27, 4652-4658.

169 Ali S. (1983) *J. Phys. Chem.*, 137, 13-21.

170 Haschets C.W. and Shine A.D. (1993) *Macromolecules*, 26, 5052-5060.

171 Heller J.P. and Dandge D.K. (1985) *Soc. Pet. Eng. J.*, 25, 679-86.

172 Chiou J.S., Barlow J.W. and Paul D.R. (1985) *J. Appl. Polym. Sci.*, 30, 2633-2642.

173 Wissinger R.G. and Paulaitis M.E. (1991) *J. Polym. Sci., Part B: Polym. Phys.*, 29, 631-639.

174 Condo P.D. and Johnston K.P. (1992) *Macromolecules*, 25, 6730-6732.

175 Hachisuka H., Sato T. and Imai T. (1990) *Polym. J.*, 22, 77-79.

Final manuscript received in December 1997